

University of New Hampshire
University of New Hampshire Scholars' Repository

Master's Theses and Capstones

Student Scholarship

Winter 2009

Identification of *Photorhabdus temperata* motility mutants altered in insect pathogenesis

Holli N. Rowedder

University of New Hampshire, Durham

Follow this and additional works at: <https://scholars.unh.edu/thesis>

Recommended Citation

Rowedder, Holli N., "Identification of *Photorhabdus temperata* motility mutants altered in insect pathogenesis" (2009). *Master's Theses and Capstones*. 506.

<https://scholars.unh.edu/thesis/506>

This Thesis is brought to you for free and open access by the Student Scholarship at University of New Hampshire Scholars' Repository. It has been accepted for inclusion in Master's Theses and Capstones by an authorized administrator of University of New Hampshire Scholars' Repository. For more information, please contact nicole.hentz@unh.edu.

IDENTIFICATION OF *PHOTORHABDUS TEMPERATA* MOTILITY MUTANTS
ALTERED IN INSECT PATHOGENESIS

BY

HOLLI N. ROWEDDER
B.S., Lock Haven University of Pennsylvania, 2007

THESIS

Submitted to the University of New Hampshire
in Partial Fulfillment of
the Requirements for the Degree of

Master of Science
in
Microbiology

December, 2009

UMI Number: 1481709

All rights reserved

INFORMATION TO ALL USERS

The quality of this reproduction is dependent upon the quality of the copy submitted.

In the unlikely event that the author did not send a complete manuscript and there are missing pages, these will be noted. Also, if material had to be removed, a note will indicate the deletion.



UMI 1481709

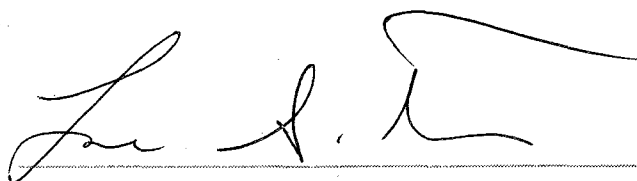
Copyright 2010 by ProQuest LLC.

All rights reserved. This edition of the work is protected against unauthorized copying under Title 17, United States Code.

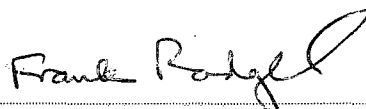


ProQuest LLC
789 East Eisenhower Parkway
P.O. Box 1346
Ann Arbor, MI 48106-1346

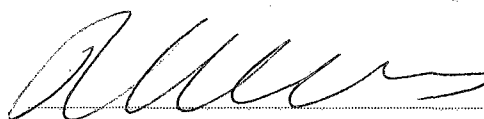
This thesis has been examined and approved.



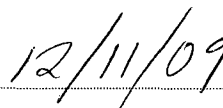
Thesis Director, Louis S. Tisa, Professor of
Microbiology and Genetics



Frank Rodgers, Professor of Microbiology



W. Kelley Thomas, Professor of Biochemistry



Date

ACKNOWLEDGMENTS

Funding for this project was provided in part by Hatch AES 702, USDA NRI 2009-35302-05257, UNH COLSA, and the Graduate School TA Fellowship. Thank you to my committee members, Louis Tisa, Frank Rodgers, and Kelley Thomas for their constant guidance and support. A special thanks goes to my thesis director, Dr. Tisa, for his patience and for giving me this opportunity. I feel lucky to be a member of his lab.

Many thanks go to all members of the Tisa Lab, past and present, for their assistance and friendship. Brandeye Michaels, Ryan Jacobeck and Erik Janicki, who generated and screened the mutant library, laid the groundwork for this project. Jon Gately completed symbiosis and calcofluor screens. I could not have completed this research without the help of undergraduates for countless injections and assays. Thank you, Noel Alaka, Bryan Ballard, Ben Bailey, Hannah Bullock, and Kate Pereira. Special thanks to Jon Gately for his work, as well as his never-ending "optimism" and support. Thank you Sheldon Hurst IV and Christine Chapman for helping me finish labwork in the very end.

Thanks goes to the Graduate school, the MCBS department and the Microbiology program. Thanks to Robert Mooney and Nick Beauchemin, for their ever-ready technical support and advice. To my fellow graduate students, it is their friendships that have made grad school almost enjoyable, especially Laura Benton and Megan Striplin.

Finally, thank you to my family: My amazing parents, Mark and Martha, my sister, Kelli, and my friend that we consider family, Kate Oechler. I could not be here today without their unyielding love and support.

TABLE OF CONTENTS

<u>ACKNOWLEDGMENTS</u>	<u>III</u>
LIST OF FIGURES	VI
LIST OF TABLES	VII
<u>ABSTRACT</u>	<u>VIII</u>
<u>CHAPTER I</u>	<u>1</u>
INTRODUCTION	1
<u>ENTOMOPATHOGENS AS BIOLOGICAL CONTROLS</u>	1
<u>PHOTORHABDUS SPECIES</u>	4
<u>PHOTORHABDUS-HETERORHABDITIS SYMBIOSIS</u>	5
<u>INSECT PATHOGENESIS</u>	7
<u>MOTILITY IN PHOTORHABDUS INFECTIONS</u>	11
<u>RESEARCH BACKGROUND AND GOALS</u>	12
<u>CHAPTER II</u>	<u>15</u>
METHODS AND MATERIALS	15
<u>STRAINS AND GROWTH CONDITIONS</u>	15
<u>PHYSIOLOGICAL ASSAYS</u>	15
<u>AXENIC NEMATODE CULTURES</u>	21
<u>SYMBIOSIS ASSAY</u>	22
<u>INSECT MORTALITY ASSAYS</u>	23
<u>MOLECULAR BIOLOGY</u>	24
<u>GENUS VERIFICATION</u>	25
<u>SOUTHERN HYBRIDIZATION</u>	28
<u>ARBITRARY PCR</u>	29
<u>GENE SEQUENCING</u>	30
<u>P. TEMPERATA NC19 GENOME DRAFT SEQUENCE</u>	31
<u>CONFIRMATION OF GENE IDENTIFICATION</u>	31
<u>RNA EXTRACTION AND DNASE TREATMENT</u>	31
<u>RT-PCR AND cDNA SYNTHESIS</u>	32
<u>GENETIC COMPLEMENTATION</u>	33
<u>EXPRESSION OF COMPLEMENTED MUTANTS</u>	35
<u>CHAPTER III</u>	<u>37</u>
RESULTS	37
<u>IDENTIFICATION OF PATHOGENESIS MUTANTS</u>	37
<u>CONFIRMATION OF PATHOGENESIS MUTANTS</u>	40
<u>IDENTIFICATION OF SYMBIOSIS MUTANTS</u>	42

<u>CONFIRMATION OF SYMBIOSIS MUTANTS</u>	44
<u>PHENOTYPIC CHARACTERIZATION OF PATHOGENESIS AND SYMBIOSIS MUTANTS</u>	44
<u>MOLECULAR CHARACTERIZATION OF PATHOGENESIS AND SYMBIOSIS MUTANTS</u>	49
<u>GENETIC COMPLEMENTATION OF UNH1307</u>	53
<u>CHAPTER IV</u>	<u>63</u>
<u>DISCUSSION</u>	<u>63</u>
<u>USE OF MOTILITY AND CALCOFLUOR-BINDING MUTANTS FOR PATHOGENESIS STUDY</u>	63
<u>INSECT MORTALITY SCREEN INDICATE ALL OF THE MUTANTS TESTED WERE VIRULENT</u>	67
<u>ALL SCREENED MUTANTS WERE CAPABLE OF NEMATODE SYMBIOSIS</u>	68
<u>MOTILITY IS NOT RELATED TO THE INFECTION OF INVERTEBRATE HOSTS</u>	69
<u>SECONDARY PHASE CHARACTERISTICS FOR PRIMARY PHASE CELL MUTANTS</u>	71
<u>CALCOFLUOR MUTANT, UNH2033, IDENTIFIED WITH DELAYED PATHOGENESIS</u>	72
<u>UNH1307 IS A RNASEII MUTANT</u>	73
<u>UNH6441 AND UNH6427: SAME GENE, DIFFERENT PHENOTYPES</u>	75
<u>SIGNIFICANCE</u>	76
<u>REFERENCES</u>	<u>78</u>
<u>APPENDIX</u>	<u>85</u>

LIST OF FIGURES

- FIGURE 1: THE *HETERORHABDITIS-PHOTORHABDUS* LIFECYCLE
- FIGURE 2: THE AMPLIFICATION OF *PTE2811*
- FIGURE 3: *IN VIVO* INSECT PATHOGENESIS ASSAYS REVEALED MUTANTS WITH REDUCED AND ENHANCED INSECT VIRULENCE
- FIGURE 4: VERIFICATION OF MUTANTS EXHIBITING ALTERED VIRULENCE
- FIGURE 5: MUTANTS WERE SCREENED FOR SYMBIOSIS IN A 24-WELL TEST PLATE CONTAINING LIPID AGAR
- FIGURE 6: ANTIBIOTIC ACTIVITY PHYSIOLOGICALLY CHARACTERIZED INTERESTING MUTANTS
- FIGURE 7: A SINGLE INSERTION OF THE MINI-Tn5 TRANSPOSON DETERMINED BY A SOUTHERN HYBRIDIZATION
- FIGURE 8: A PCR APPROACH CONFIRMED ARBITRARY PCR SEQUENCING RESULTS
- FIGURE 9: THE *PHR1* CONSTRUCT WITH A *pBAD18* BACKBONE
- FIGURE 10: GENETIC COMPLEMENTATION AND EXPRESSION OF *PTE2811* WAS VERIFIED THROUGH CDNA SYNTHESIS AND END-POINT RT-PCR
- FIGURE 11: GENETIC COMPLEMENTATION RESTORES SWIMMING BEHAVIOR IN UNH1307
- FIGURE 12: ARABINOSE WAS NOT REQUIRED FOR RESTORED SWIMMING BEHAVIOR FOR UNH1307
- FIGURE 13: GENETIC COMPLEMENTATION RESTORES VIRULENCE IN UNH1307
- FIGURE 14: GENETIC COMPLEMENTATION OF UNH1307 PARTIALLY RESTORES ANTIBIOTIC ACTIVITY
- FIGURE 15: GENOMIC COMPARISONS OF 10 GENOMES OF INTEREST
- FIGURE 16: ORTHOLOGS UNIQUE TO SPECIFIED GENOMIC GROUPS AND FURTHER DETERMINED AS PROTEINS OF CHARACTERIZED OR UNKNOWN FUNCTIONS
- FIGURE 17: PROPOSED CONSENSUS PHYLOGENETIC TREES BASED ON 246 ORTHOLOGS

LIST OF TABLES

TABLE 1: STRAINS AND PLASMIDS USED IN THIS STUDY

TABLE 2: PRIMERS USED IN THIS STUDY

TABLE 3: PHYSIOLOGICAL CHARACTERIZATION OF SELECTED TRANSPOSON MUTANTS

TABLE 4: GENETIC IDENTIFICATION OF SELECTED TRANSPOSON MUTANTS

TABLE 5: GENETIC COMPLEMENTATION OF UNH1307 RESTORES WILD-TYPE
CHARACTERISTICS

TABLE 6: GENES OF INTEREST UNIQUE TO SPECIFIED GENOMIC GROUPS

TABLE 7: THE PRESENCE OR ABSENCE OF KEGG ASSOCIATED GENES IN EACH GENOME

ABSTRACT

IDENTIFICATION OF *PHOTORHABDUS TEMPERATA* MOTILITY MUTANTS ALTERED IN INSECT PATHOGENESIS

by

Holli N. Rowedder

University of New Hampshire, December 2009

The entomopathogenic nematode *Heterorhabditis bacteriophora* forms a specific association with its bacterial partner *Photorhabdus temperata*. The objective of this study was to identify genes involved in insect pathogenesis. Previously we generated a bank of 10,000 transposon mutants and identified 86 motility mutants and 11 calcofluor-binding mutants. The purpose of these experiments was to determine the effects of these defects on bacterial pathogenesis and mutualism. An insect mortality screen with host-model, *Galleria mellonella*, initially identified 14 mutants with altered insect pathogenesis. Four mutants were confirmed including one (UNH5832) with an enhanced pathogenesis response compared to the parental wild-type, while three other mutants (UNH1307, UNH6441, UNH2033) exhibited a delayed response that was not related to growth rate. These verified mutants include 3 defective motility mutants and one calcofluor-binding mutant. Genetic complementation of UNH1307 proved RNase II to have pleiotropic effects in *P. temperata*, including the regulation of virulence and motility.

CHAPTER I

INTRODUCTION

Entomopathogens as Biological Controls

Every year worldwide, insect pests cause billions of dollars in damage to crops, turf-grass, and ornamental landscaping. In the US, millions of dollars are spent to prevent or repair damage. As chemicals seep into food chains and water supplies, non-targeted organisms have been affected. With the increased health concerns of chemical pesticides, society is demanding eco-friendly alternatives. Biological control agents hold great promise to attack insect pests and without harming the environment (Chattopadhyay et al, 2004). One type of naturally-occurring insect biological control is found within two families of entomopathogenic nematodes: *Steinernematidae* and *Heterorhabditidae*. These nematodes have evolved a specific mutualistic relationship with entomopathogenic bacteria of the genera, *Xenorhabdus* and *Photorhabdus*, respectively (Goodrich-Blair & Clark, 2007; Ansari et al, 2002). A unique aspect of these bacteria is that they are virulent to many invertebrate hosts, but are symbiotic to these specific nematodes (Figure 1). Other nematode competitors are controlled by antinematicidal compounds produced during the life cycle of the bacteria. The bacteria are carried in the gut of an infective juvenile (IJ), which infect a broad range of insect prey (Clarke, 2008; Hallem et al, 2007). After entering the insect, the nematode regurgitates bacteria into the hemocoel, where

the bacteria rapidly replicate and produce a multitude of virulence factors, extracellular hydrolytic enzymes, and antibiotics. Within 48 h *Photorhabdus* or *Xenorhabdus* successfully evades the host's defensive systems and kills the insect by toxemia and septicemia, while converting the insect cadaver into nutrients for nematode development (Waterfield et al 2009; Clarke, 2008; Hallem et al, 2007; Bennett & Clarke, 2005; Ciche & Ensign, 2003; Boemare, 2002). The bacteria-nematode symbiosis may be described as a cyclic event, both beginning and ending with infective juveniles in the soil (Forst & Clarke, 2002).

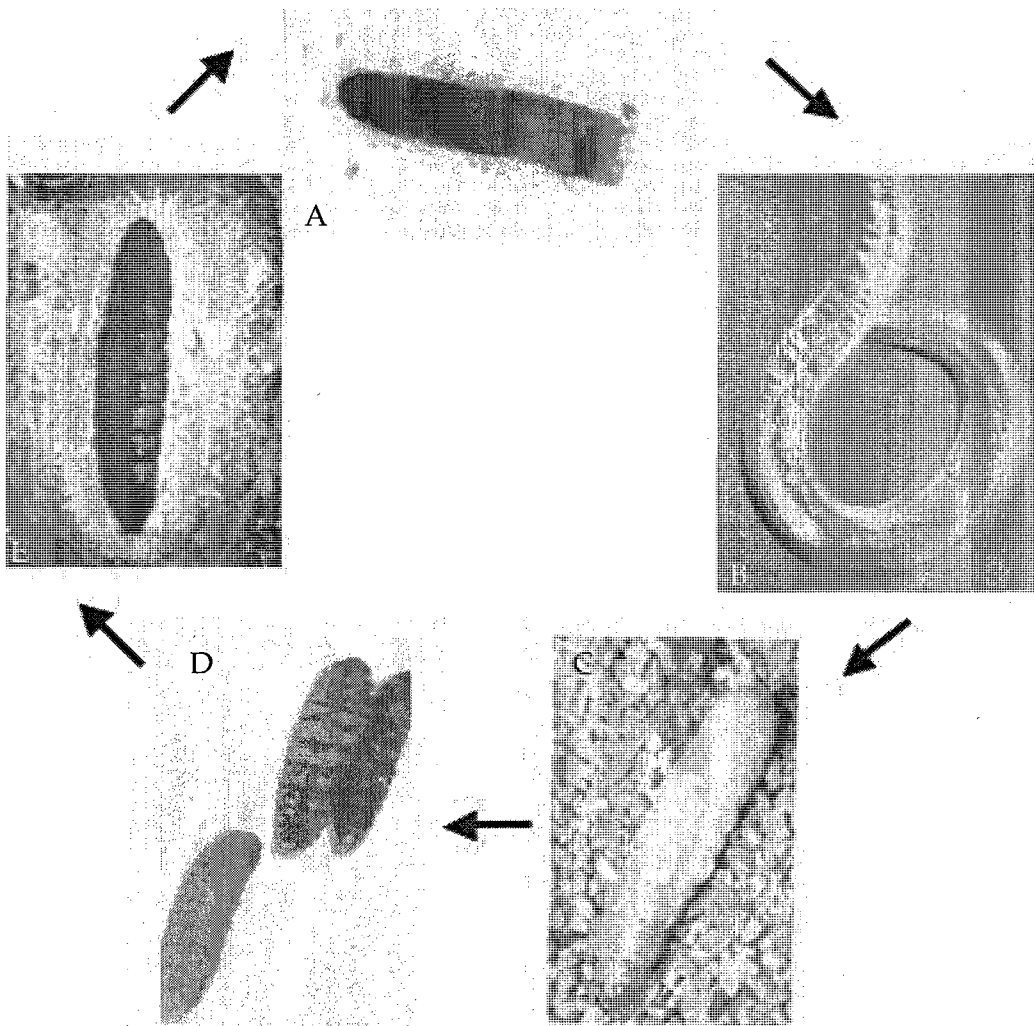


Figure 1. The *Heterorhabditis-Photorhabdus* lifecycle. (A) *Photorhabdus* cells (B) colonize the midgut of a *Heterorhabditis* Infective Juvenile. (C) IJs actively seek out insect prey and enter into the hemolymph. (D) *Photorhabdus* kills the insect within 48 h with a myriad of virulence factors. (E) After several nematode generations, over 100,000 infective juveniles are released from the insect cadaver.

Photorhabdus species

Photorhabdus spp. are gram-negative bacteria belonging to the *Enterobacteriaceae* family. These bacteria are facultative anaerobes and highly motile by means of peritrichous flagella (Clarke, 2008; Boemare, 2002). Re-classified from the closely-related genus *Xenorhabdus*, *Photorhabdus* is the only known terrestrial bacteria exhibiting bioluminescence (Waterfield et al, 2009; Joyce et al, 2006; Tounsi et al, 2006).

Photorhabdus are classified taxonomically into three species: *P. luminescens*, *P. temperata*, and *P. asymbiotica*, with several subspecies to date (Taillez et al, 2009; Tounsi et al, 2006). The complete genome sequence for *P. luminescens* strain TT01 (Duchard et al, 2003) and *P. asymbiotica* strain ATCC43949 (http://www.sanger.ac.uk/Projects/P_asymbiotica/) are available. The complete genome of *P. temperata* strain NC19 is currently being finished (L.S. Tisa, unpublished). All of these species are insect pathogens, and have symbiotic relationships with specific species of *Heterorhabditidae* (Waterfield et al, 2009; Boemare, 2002).

P. asymbiotica, is an emerging human pathogen, known to cause localized primary infections in skin or soft tissues and disseminated bacteremic infections (Costas et al, 2009; Gerrard et al, 2004; Weissfield et al, 2005). Initially, *P. asymbiotica* isolates obtained from clinical cases in Australia and the US were believed to exist as free-living forms without a nematode host, and hence the species name. However, Gerrard et al (2006) discovered the *Heterorhabditis* nematode symbiotic host and disproved that hypothesis. Though *P. asymbiotica* is unique in the aspect of mammalian pathogenesis, all *Photorhabdus* species

undergo a similar lifecycle including insect pathogenicity and nematode symbiosis. (Waterfield et al, 2009).

Photorhabdus exists in two phenotypic phase-variant stages known as the primary- and secondary-phase (Derzelle et al, 2004; Boemare & Lanois, 1997; Akhurst, 1980). The two phase variants are easily identified by several phenotypic traits including dye absorption, and colonial and cellular morphology. Primary-phase cells occur naturally in symbiosis with nematodes, and exhibit higher amounts of antibiotics, lipases, phospholipases, proteases, pigmentation and bioluminescence than the secondary-phase variant (Gaudriault et al, 2008; Derzelle et al, 2004; Forst & Neilson, 1996). Although both phase variants are equally virulent, the secondary phase variant is far less effective at providing conditions to support nematode growth, development and reproduction (Waterfield et al, 2009; Boemare, 2002). The ecological importance and mechanics of this phase variation are unknown, but conversion from Phase I to II will occur spontaneously under nutrient-limited *in vitro* culturing and appears to be unidirectional. (Waterfield et al, 2009; Derzelle et al, 2004; Boemare, 2002; Boemare et al. 1997).

***Photorhabdus-Heterorhabditis* symbiosis**

IJs are a non-feeding nematode stage that are resistant to environmental stresses and are induced by nutrient depletion (Hallem et al, 2007; Forst & Clarke, 2002; Burnell & Stock, 2000). *Photorhabdus* is carried within a specific midgut region of the *Heterorhabditis* nematode. The pair interaction between *Photorhabdus* and *Heterorhabditis* is highly specific. One strain of nematode

retains only one bacterial species. Within the nematode gut, adhering cells form persistent biofilms, while other symbiotic bacterial cells are transiently present in the intestine (Waterfield et al, 2009; Ciche et al, 2008). IJs actively seek insect hosts and enter through natural orifices or use a tooth-like appendage to enter through the cuticle. Once in the hemocoel, the nematode regurgitates every bacterial cell (50-200 cells). A switch to feeding behavior initializes “recovery” and the nematode develops into a self-fertilizing hermaphrodite (Waterfield et al, 2009; Forst & Clarke, 2002). The environmental conditions provided by the bacteria and insect determine the developmental pathway of *Heterorhabditis*. Uncharacterized signal molecules within the insect and a food signal from the bacteria, stimulate IJ recovery. One component of this food signal is 3,5-dihydroxy-4-ethylstilbene (ST), a major secondary metabolite produced by *Photorhabdus* and required for nematode growth and development (Waterfield et al, 2009). This molecule is derived from the head-to-head condensation of two-ketoacyl thioesters. *Photorhabdus* is the only known organism outside of the plant kingdom to produce ST (Bode, 2009; Joyce et al, 2008). Normal nematode development is also dependent on exogenous sterols found within the insect. As an adaptation for symbiosis, *Photorhabdus* produces a significant amount of iso-branched fatty acids, more so than other members of *Enterobacteriaceae* (Waterfield et al, 2009). Iron is another essential nutrient for nematode growth and development and different nematode species have different iron needs. This iron requirement could be a factor in the species specificity of the nematode-bacteria symbiosis (Clarke, 2008).

With adequate developmental factors, nematodes will transition through four larval stages (L1-L2-L3-L4) before developing into a male or female adult.

(Ciche et al, 2008; Hallem et al, 2007; Burnell & Stock, 2000). While in the insect cadaver, nematodes undergo several generations over the period of 1-3 weeks. During this time, *Photorhabdus* maintains the insect cadaver free of invaders and indigenous microbiota through the production of a multitude of wide spectrum antimicrobial, antinematocidal, and antifungal agents (Waterfield et al, 2009). For example, the ST molecule is effective against insect gut bacteria, and also inhibits fungi and other scavenging organisms including free-living nematodes like *Cenorhabditis elegans* or even some strains of *Steinernema* (Waterfield et al, 2009; Bode, 2009; Forst & Clarke, 2002). In addition to ST and small-molecule antibiotics, *Photorhabdus* produces an array of antibacterial protein molecules including S and R-type pyocins (Waterfield et al, 2009).

Bacteria grow to high cell densities within the nutrient-rich insect hemocoel, and this nutrient depletion signals IJ formation. Similar to the dauer stage of *C. elegans*, IJ formation is an alternative route of development initiated by environmental cues (Hallem et al, 2007; Forst & Clarke, 2002; Burnell & Stock, 2000). In entomopathogenic nematodes, IJ formation is crucial to the lifecycle and occurs after the third stage (L3) of development (Clarke, 2008; Forst & Clarke, 2002). *Photorhabdus* is still at high population density within the insect cadaver when the bacteria re-colonize the gut suggesting a complex set of signals for the process. Once colonized by the bacteria, several thousand IJs are released from the cadaver and leave in search of new prey.

Insect Pathogenesis

Intrinsically coupled in nature, mutualism is a prerequisite requirement for insect pathogenesis. *Photorhabdus* has evolved to be an extremely virulent

organism, killing its prey with as little as one colony forming unit (Goodrich-Blair & Clarke, 2007; Joyce et al, 2006; Clarke & Dowds, 1995). Analysis of *Photorhabdus* genome revealed the presence of genes encoding proteins similar to virulence factors in a wide range of mammalian pathogens (Duchard et al 2003; French-Constant et al, 2000; Forst & Clarke, 2002). Over 2000 genes had an ortholog in *Yersinia pestis*, which has a similar lifecycle.

To be an effective pathogen, *Photorhabdus* must overcome a fast-acting insect immune response. This sophisticated system functions cooperatively and exhibits both humoral and cellular components (Waterfield et al, 2009). Humoral response involves the rapid production of lysozymes, proteases, free radicals and antimicrobial peptides upon initial infection (Waterfield et al, 2009; Forst & Clarke, 2002). Antimicrobial peptides (AMPs) are competent and widespread and include a metalloproteinase inhibitor, transferrin, galiomicin, and gallerimycin. Insects would quickly succumb to infection without the signal-dependent synthesis of AMPs (Kavanagh & Reeves, 2007). Hemocytes function similar to mammalian neutrophils and are a central component to the cellular response. Hemocytes are rapidly synthesized and mobilized to engulf, internalize, and destroy invading microorganisms (Kavanagh & Reeves, 2007). After being released into the insect hemocoel, bacterial growth is exponential and unhindered (French-Constant et al, 2003). Although insect host immune responses differ, host serum can cause a release of lipopolysaccharide (LPS) from the outer membrane. This alteration induces a rapid increase in hemocytes, resulting in hemocyte damage. LPS has cytotoxic effects via the binding of fatty acids of the lipid A moiety to the glucosaminyl receptors on the hemocytes (Clarke, 2008; Dowds & Peters, 2002). As a result of this hemocyte damage, LPS

inhibits the activation of the prophenoloxidase cascade, another part of the insect immune response (Dowds & Peters, 2002). This cascade is activated by the coordinated response of hemocytes, called nodulation, where layers of hemocytes envelop a large invading organism, such as a nematode. The prophenoloxidase cascade deposits a layer of melanin around the invading organism (Waterfield et al, 2009; Forst & Clarke, 2002). Stilbenes also play a role in inhibiting the prophenoloxidase cascade (Bode, 2009). Additionally, *Photorhabdus* contains highly conserved components of the Type III Secretion System (TTSS), which are used to deliver effector molecules into host cells to alter cell behavior (Brugirard-Ricaud et al, 2004; ffrench-Constant et al, 2003). This TTSS system has been shown to secrete LopT protein, which is a homologue of YopT and YopR proteins from *Y. pestis* (Joyce et al, 2006). This protein appears to be necessary for infection and possibly inhibits phagocytosis (Clarke, 2008). YopT functions to uncouple RhoA-effector interactions suggesting that this secretion system will rearrange the cytoskeleton altering the behavior of hemocytes (ffrench-Constant et al, 2003).

Once established within the insect, bacterial virulence is mostly due to extracellularly excreted insect toxins (i.e. prtA or the tc toxin complex) and other factors including a metalloprotease. These virulence factors are highly secreted gut-active toxins that cause a rapid destruction of the insect gut (Waterfield et al, 2009; Marokhazi et al, 2003; Daborn et al, 2002). Due to the multiple copies of the tc genes within individual *Photorhabdus* strains, several different Tc toxins are hypothesized to be produced and are effective against different tissues within individual hosts or effective against different insect hosts (ffrench-Constant et al, 2003). *Photorhabdus* also produces a toxin encoded by the *makes caterpillar floppy*

(*mcf*) gene (Daborn et al, 2002). The *mcf* toxin is taken up by endocytosis by an unknown mechanism and induces apoptosis of the hemocytes and midgut epithelium. This cell death causes a rapid loss of body turgor pressure resulting in the “floppy” phenotype. (Daborn et al, 2002; Dowling et al, 2004).

Besides extracellular toxins, a number of extracellular enzymes have been examined for their roles of virulence. Several enzymes have a direct effect on virulence, while others work in collaboration with other factors (Dowds & Peters, 2002). Lipase activity, which has been implicated in many pathogens, appears to act by directly attacking host tissues, evading immune response or nutrient acquisition (Richards et al, 2008). Hemolysins, named for their activity against mammalian red blood cells, are another example of redundant virulence factors at the disposal of *Photorhabdus*. *Photorhabdus* produces an annular hemolysis on sheep’s blood, an unusual type of hemolysis showing a partial hemolysis immediately around the colony and a thin line of complete hemolysis at some distance from the colony (Brillard et al, 2001). This action is not limited to the clinical strain, *P. asymbiotica*, but seen in the insect pathogens as well. As insects do not contain red blood cells, hemolysins are utilized to lyse insect humoral cells. In *Xenorhabdus*, hemolysins are crucial for full virulence and are capable of targeting specific immune cells. It is unknown whether this effect is the result of protection against immune cells or nutrient acquisition from hemocytes. Expression of hemolytic activity is induced in iron-limiting environments, suggesting a potential role for hemolysins in iron acquisition. This role, however, would have no effect in an insect host. (Cowles & Goodrich-Blair, 2005; Brillard et al, 2001). Examinations of the fully sequenced genomes do not result in any mammalian-only virulence factors. This supports the idea that insect evolved

virulence factors, such as hemolysins, play a particular role in insect virulence but are readily deployed against mammalian hosts (Waterfield et al, 2009).

Motility in *Photorhabdus* infections

Although not a specific part of the lifecycle, motility is an important factor in the *Photorhabdus-Heterorhabditis* lifecycle (Waterfield et al, 2009; Joyce et al, 2006; Dowds & Peters, 2002). Bacteria move in a synchronized fashion, towards attractants and away from repellents (Hodgson et al, 2003). A combination of motility and chemotaxis allow the organism to attain nutrients and to reach and colonize a certain niche (Josenhaum and Suerbaum, 2002). Under the appropriate conditions, primary and secondary phase *Photorhabdus* cells are motile (Hodgson et al, 2003). These bacteria exhibit three types of movements: surface movement (swarming), liquid movement (swimming) and twitching (Michaels, 2006). For swimming, motility is driven by the rotation of peritrichous flagella and was comprehensively studied (Hodgson et al 2003, Micheals 2006). One unusual feature of *Photorhabdus* motility is a salt requirement for flagella formation. Sufficient levels of Na⁺ or K⁺ ions are required for flagella biosynthesis and formation (Hodgson et al, 2003). Microarray and immunoblotting experiments indicated that Na⁺ and K⁺ regulate flagella biosynthesis post-transcriptionally and at the transcriptional level (Michaels, 2006).

Photorhabdus uses the same flagella system for swimming and swarming motility (Micheals 2006). Several lines of evidence supported this idea. Medium constituents especially agar concentrations affected swarming motility. Swarming is better on low agar concentrations with 0.65 % being optimal. As the

agar concentrations increase, swarm ring diameters decreased. Unlike swimming, swarming behavior is a social form of movement in which the cells coordinately form intricate channels covering the surface. These appendages are composed of cells that are aligned next to each other. The cells moved forward and backward, but do not exhibit tumbling or angular motion found with swimming behavior.

Motile organisms spend considerable energy in synthesizing a flagellar apparatus and providing the energy for movement. In most cases, the cost associated with the production of flagella is offset by the ability to be motile within the host (Easom and Clarke, 2008; Josenhaum and Suerbaum, 2002). Motility has been tied to the virulence of many mammalian pathogens as well as the colonization of symbionts (Josenhaum and Suerbaum, 2002; Graf et al, 1994). Several cases have shown that not necessarily motility is required for full virulence, but appropriate flagellar expression is needed, as non-flagellated mutants show reduced virulence (Josenhaum and Suerbaum, 2002; Givaudan & Lanois, 2000; Graf et al, 1994). In a number of species, flagellum-mediated motility appears to play different roles in host interactions. Although motility or flagella are not required for pathogenicity or mutualism of *Photorhabdus*, motility does contribute to the competitive fitness during infection of both the insect and the nematode. Studies show a significant advantage to being motile during the prolonged incubation with the insect (Easom & Clarke, 2008).

Research Background and Goals

Michaels (2006) used a genetic approach to understand the role of motility and biofilm formation in nematode symbiosis and insect pathogenesis. A

collection of transposon mutants was generated for *P. temperata* NC19 and used the mini-Tn5 system of Ciche et al (2001). A bank of 10,000 primary-phase mutants was developed and screened for motility defects (Michaels et al, 2004; Michaels, 2006). This screen of the entire library identified 86 motility mutants, which were isolated and further characterized. These motility mutants are classified into five categories: (1) 33 hyperswarmers, (2) 12 hyperswimmers, (3) 23 nonmotiles, (4) 12 mutants with defective/aberrant swimming, and (5) 6 mutants capable of swimming without salt.

Hyperswarmers exhibit faster swarming rates and form larger swarm rings than the parental wild-type. These mutants will swarm on swarm medium containing higher (1%) agar concentration that inhibits swarming by wild-type cells. Hyperswimmers form swim rings in swim media noticeably earlier than the parental wild-type. Nonmotile mutants are easily identified as a compact colony formation on swim media, which exhibits no swim rings. *P. temperata* requires additional NaCl or KCl to produce flagella and be motile (Hodgson et al, 2003). Another class of mutants is capable of swimming in swim media lacking additional salt. The last class of mutants has aberrant or defective motility. Although these mutants are motile, any swim ring formation is greatly reduced forming smaller and/or oddly-shaped swim rings. The genetic and physiological properties of these mutants were only briefly examined, but serve as a foundation for the present study.

Besides motility, the transposon mutant library was also screened for calcofluor-binding (Gately, Janicki, and Tisa, Unpublished). Calcofluor white is a fluorescent dye that binds to acidic residues in the exopolysaccharides of several different bacterial species and has been used to identify mutants defective in the

production of exopolysaccharides including *Rhizobium meliloti* (Leigh et al, 1985) and *Myxococcus xanthus* (Ramaswamy et al, 1997). *Photorhabdus* secondary-phase cells are able to bind calcofluor, while primary-phase cells do not bind the dye (E. Janicki and L.S. Tisa, unpublished). A total of 11 primary phase mutants are capable of binding calcofluor, indicating an altered cell surface. One of these mutants (UNH7695) is also defective in motility.

The overall goal of this research was to identify genes responsible for *Photorhabdus temperata* virulence in mutants featuring altered motility. Building off the previous studies in the Tisa laboratory, the *P. temperata* motility and calcofluor-binding mutants identified in the transposon mutant library were used a starting point to elucidate genes involved in pathogenesis (Michaels et al, 2004; Michaels, 2006). The first goal of this research was the identification of mutants with altered virulence. Since the *in vivo* insect pathogenesis assay is very labor intensive, screening was restricted to the above subset of mutants (motility and calcofluor-binding mutants). Pathogenesis mutants were identified by screening in the insect model system, *Galleria mellonella*. The second goal of the project focused molecular, genetic and physiological characterization of the identified pathogenesis mutants. The last goal of this project was to show causality of the transposon-disrupted gene by genetically complementing one of the mutants.

CHAPTER II

METHODS AND MATERIALS

Strains and Growth Conditions

For this study, primary and secondary phase variants of *Photorhabdus temperata* strain NC19 (ATCC 29304) and a transposon mutant library of primary phase cells were used. The mini-Tn5 mutant library was generated as described previously (Michaels 2006). Table 1 lists all of the bacterial strains and plasmids used in this study. Cultures were grown and maintained in Luria-Bertani (LB) medium [1% Bacto-Tryptone (Difco Laboratories), 0.5% yeast extract, 0.5% NaCl] at 28°C and supplemented kanamycin (25 µg/ml) when needed.

Physiological Assays

A series of phenotypic assays were used to distinguish between primary and secondary phase cells and fully characterize the transposon mutants.

Dye absorption For each subculture, phase status was identified by pigmentation and by differential dye absorption (Boemare et al, 1997). In this study, differential dye absorption of neutral red and eosin Y was used. Strains were grown at 28°C for 48 h on MacConkey (Difco Laboratories, Sparks, MD) and Eosin Blue [2% Proteose Peptone 3 (Difco Laboratories), 1% Bacto-Agar (Difco Laboratories), 0.4% Eosin Y, 0.067%

Table 1. Strains and plasmids used in this study.

Strains	Strains or Plasmids	Relevant genotype / characteristics	Source or Reference
<i>Escherichia coli</i>			
DH5a	General cloning strain		Labstock
MG 1665	Indicator culture		Labstock
TOP10	General cloning strain		Invitrogen
<i>Micrococcus luteus</i>	Indicator culture		Labstock
<i>Staphylococcus aureus</i>	Indicator culture		Labstock
<i>Bacillus subtilis</i> 168	Indicator culture		Labstock
<i>Photobacterium temperata</i>			
NC19 (ATCC29304) 1°	Parental wild-type; Calcofluor -		
NC19 (ATCC29304) 2°	Secondary variant of wild-type; Calcofluor+ wild-type; axenic nematodes		
Meg1	Hyperswarmer; Kan ^R		Michaels, 2006
UNH1201	Defective motility; Kan ^R		Michaels, 2006
UNH1307	Calcofluor; Kan ^R		Michaels, 2006
UNH2033	Nonmotile; Kan ^R		Michaels, 2006
UNH2072	Hyperswarmer; Kan ^R		Michaels, 2006
UNH5006	Defective motility; Kan ^R		Michaels, 2006
UNH5832	Hyperswarmer; Kan ^R		Michaels, 2006
UNH6290	Defective motility; Kan ^R		Michaels, 2006
UNH6427	Defective motility; Kan ^R		Michaels, 2006
UNH6441	Defective motility; Kan ^R		Michaels, 2006
UNH7504	Defective motility; Kan ^R		Michaels, 2006
UNH8178	Hyperswarmer; Kan ^R		Michaels, 2006
UNH8191	Hyperswarmer; Kan ^R		Michaels, 2006

Table 1 Continued

UNH8309	Defective motility; Kan ^R	Michaels, 2006
UNH8322	Hyperswarmer; Kan ^R	Michaels, 2006
UNH8678	Defective motility; Kan ^R	Michaels, 2006
UNH8776	Nonmotile; Kan ^R	Michaels, 2006
UNH9304	Defective motility; Kan ^R	Michaels, 2006
HNR0018	Parental WT with pBAD18; Cm ^R	This study
HNR0606	Parental WT with pHR1; Cm ^R	This study
HNR1318	UNH1307 with pBAD18; Kan ^R ; Cm ^R	This study
HNR1307	UNH1307 with pHR1; Kan ^R ; Cm ^R	This study
Nematode strain		
Heterorhabditis bacteriophora strain NC1		
P. Stock		
Plasmids		
pCR2.1-TOPO	General cloning vector; Amp ^R ; Km ^R	Invitrogen
pUB394	mini-Tn5 delivery vector; Kan ^R , Str ^R , Spec ^R	Ciche, 2001
pBAD18-Cm	vector; arabinose-inducible promoter; Cm ^R	Guzman, 1995
pHR1	pBAD18 containing <i>pie2811</i> ; Cm ^R	This study

Methylene Blue] media. Primary variant colonies are red or purple with a green sheen on MacConkey or EB plates, respectively, while secondary variant colonies are off-white or light purple. On LB medium, primary-phase-variant strain NC19 colonies were pigmented (yellowish-orange) while secondary-phase-variant colonies were off-white.

DNase DNase activity was assayed on DNase test agar containing methyl green (Difco Laboratories). Plates were spot inoculated with 10 μ l overnight broth cultures and incubated 24-48 h at 28°C. The ability to breakdown DNA was determined by the presence of a clear halo surrounding bacterial growth and activity was quantified by measuring the radius of the clearing zone.

Protease Protease activity was determined by the gelatin assay (Boemare et al, 1997). Overnight broth cultures were spot inoculated on the surface of protease test agar (2.3% Nutrient agar, 1.2% gelatin). Following inoculation, the plates were incubated for 24-48 h at 28°C. Protease activity was determined by measuring the radius of the resulting clearing zone.

Hemolysin assay Hemolytic activity was determined by observing a clearing surrounding the bacterial colonies cultured on a blood agar plates (T-soy agar [EM Science, Darmstadt, Germany] supplemented with 5% (v:v) sheep's blood). Overnight broth cultures (10 μ l) were spot inoculated on the surface of blood agar plates and the plates were incubated at 28°C

for 24-48 h. *Photorhabdus* strains show a characteristic annular hemolytic activity, which was quantified by measuring the radius of the clearing zone surrounding the bacterial colonies.

Lipase Lipase activity was tested on Spirit Blue test agar (Difco Laboratories) containing 0.5% (v/v) Tween 20. Overnight broth cultures (10 l) were spot inoculated on the surface of the medium and the plates were incubated at 28°C for 24-48 h. Lipase activity was determined by measuring the radius of the resulting clearing zone surrounding bacterial growth.

Antibiotic Production Assays Antibiotic activity was evaluated by placing a 5-mm-diameter plug from confluent growth of a 72-h culture of *Photorhabdus* on Proteose Peptone 3 agar medium (2% Proteose Peptone 3, 2% Bacto-agar, 0.5% NaCl) onto the surface of a LB plate that had been inoculated with an indicator culture (Table 1). After a 24-h incubation at 37°C, antibiotic activity was determined by measuring the radius of the zone of inhibition (mm).

Motility Assays Both swimming (movement in liquids) and swarming (movement of surfaces) behaviors were determined. Swimming movement was assayed with a swim-plate migration assay as previously described (Adler, 1973; Hodgson et al 2003). In this assay, a “swim migration ring” is formed as bacteria migrate in response to a gradient of amino acids created by their metabolism. Swim plates [0.5% yeast extract, 1% Bacto-peptone, 0.5% NaCl, 0.25% Bacto agar (Difco Laboratories)] were

inoculated in the center with a stab of approximately 10^6 cells and incubated at 28° C. At 24 and 48 h incubation, the diameters of the swim rings were measured. Swarming behavior was determined by spot inoculating the surface of PP3-swarm medium (2% Proteose Peptone 3 medium, 0.5% NaCl, 0.65% Bacto agar) and incubated at 28°C. The diameters of swarm rings were measured at 24 and 48 h.

Calcofluor-white Dye-Binding Assays Calcofluor white is a fluorescent dye that binds to acidic residues in the exopolysaccharides of different bacterial species and has been used to identify mutants defective in the production of exopolysaccharides including *Rhizobium meliloti* (Leigh et al, 1985) and *Myxococcus xanthus* (Ramaswamy et al, 1997). Cells binding the dye fluoresce upon exposure to UV light. *Photorhabdus* secondary-phase cells were able to bind calcofluor, while primary-phase cells did not bind the dye (E. Janicki and L.S. Tisa, unpublished). The mutants in this study were tested for the ability to bind calcofluor. For the calcofluor-white binding assay, cultures were streaked onto LB agar plates containing 0.02 mg/ml calcofluor and incubated at 28°C. The plates were exposed to UV light and examined for fluorescent colonies at 24, 48 and 72h. Cells that bound the dye fluoresced under UV light. Primary phase cultures capable of binding calcofluor while retaining primary phase characteristics would indicate an altered cell surface. Primary and secondary phase wild-type served as the negative and positive control, respectively.

Growth assay Overnight cultures were diluted in fresh LB medium to a final OD₆₀₀ of 0.01. The diluted cell cultures (150 μ l/well) were added to wells of a 96-well polystyrene microtiter plate. The inoculated plate was placed in a Tecan plate reader with Magellan software (Tecan Group Ltd., Switzerland) and incubated at 28°C with shaking. The OD₆₀₀ of the plate were determined each h for a 24 h period. The average and standard deviation of each sample was determined from the replicate wells (n= 8) and these values were plotted versus time. The doubling times were determined for the mutants and the parental primary-phase wild-type.

Axenic Nematode Cultures

Heterorhabditis bacteriophora NC1 was used for these studies. Nematode growth and propagation was performed according to modified methods of Ciche et al (2001). Growth of axenic nematodes was done on *P. temperata* Meg1, a symbiotic strain for growth and development though not retained within the gut of the nematode. Overnight cultures were plated onto lipid agar (1.6% T-soy broth, 1% yeast extract, 3% Bacto-Agar, 0.4% MgCl₂*6H₂O, 1.4% (v:v) Karo dark corn syrup, 0.8% pure corn oil) and incubated at 28°C for 24-48 h.

Approximately 10 infective juveniles (IJs) were seeded onto the plate and incubated for 10-14 days at 28°C. IJs are young nematodes that usually carry the symbiotic bacterial strain in their gut. To separate IJs from adults and hermaphrodites, 10 ml of sterile dH₂O was added to the lipid agar plate and allowed for sit at RT for 10 min. The liquid overlay containing nematodes was collected and washed several times. Nematodes were allowed to settle and supernatant was removed. The remaining nematode solution was applied to a

40 mm cell filter that was placed in a Petri dish filled with sterile dH₂O, and incubated at room temperature for 1-2 h without disruption. Standing water was collected and nematodes were harvested by centrifugation at 7,000 x g for 3 min. Nematode pellets were resuspended in 2% bleach for surface sterilization. After a 15 min incubation at room temperature, the nematodes were harvested by centrifugation at 7,000 x g for 3 min. The resulting pellet was rinsed by resuspending in sterile dH₂O and collected again. This step was repeated several times. After a final centrifugation step, the supernatant was removed to leave approximately 1 cm of sterile dH₂O above the nematode pellet and stored at 4°C and were viable for up to 2 months. Surface sterilization was verified by a bioassay. Approximately 10 IJs were homogenized in 100 μ l sterile dH₂O with a microtissue grinder. The homogenate was plated onto PP3 agar and incubated for 48 h at 28°C.

Symbiosis Assay

Screening of the ability of motility mutants to support the growth and propagation of nematodes was performed according to modified methods of Ciche et al (2001). Overnight bacterial cultures were plated onto 24-well plates containing lipid agar and grown overnight at 28°C. After overnight growth, 10-12 axenic surface-sterilized IJs were added to each well. Plates were incubated at room temperature for 21 days. Primary-phase parental wild-type NC19 and Meg1 cells served as positive controls, while secondary-phase wild-type cells acted as a negative control. Following incubation, symbiosis positive strains formed a white mass of IJs that was visible to the naked eye. Preliminary

mutants exhibiting altered symbiosis capabilities were verified on individual lipid agar plates, as described previously.

Insect mortality assays

Insect pathogenesis was tested in the greater wax moth larvae, *Galleria mellonella* according to a modified method of Clark and Dowds (1995). *G. mellonella* larvae were purchased from Grubco, Inc (Hamilton, OH) and used within 3 weeks of arrival. Larvae were stored in wood shavings at room temperature (22°C) prior to use. *P. temperata* NC19 primary-phase wild-type and mutant cultures were grown in LB medium overnight with vigorous shaking. For each sample, the OD₆₀₀ of the culture was measured by a spectrophotometer (Shidmazu Scientific Instruments, Columbia, MD). Each culture was standardized to an OD₆₀₀ of 1.0 with LB medium and further diluted 10⁵-fold. This dilution contained approximately 10 cells/μl, and 10 μl of diluted sample (about 100 cells) was directly injected into the insect hemocoel by use of a sterilized Hamilton syringe (Hamilton Company, Reno, NV). A replicate inoculum of 10 μl was spread onto LB medium containing kanamycin and 0.1% pyruvate to determine a viable cell count and also plated on MacConkey agar to determine the phase state of the cells. Two sets of controls, parental wild-type cells and sterile growth medium, were used in each experiment. All samples, including the controls, were injected in 20 larvae per sample. Larvae were incubated at room temperature and their health was monitored every 6-8 h for the duration of the assay. At these time points, insect mortality was determined. Lethal time values were determined for each mutant and compared to those values obtained with the parental wild-type. The LT₅₀ value was defined as the

time required for 50% of the larvae to die, while LT_{100} value was defined as the time required for 100% mortality. The effect of dosage, or multiplicity of infection (MOI), was determined by injecting different numbers of cells into *G. mellonella* larvae. These insects were injected as described above, but 10 μ l of the 10^{-3} to 10^{-6} dilutions were used in these assays. Insect health was monitored every 3 h and lethal time values (LT_{50} and LT_{100}) were determined for each mutant and compared to those values obtained with the parental wild-type at each dosage.

Molecular Biology

Plasmid isolations were performed using QIAprep Spin Mini Prep Kit according to the manufacturer's instructions (Qiagen Sciences, Valencia, CA). Restriction digests were performed according to recommendations of the manufacturer (New England Biolabs, Ipswich, MA). Extraction and purification of genomic DNA was completed via the cetyltrimethylammonium bromide (CTAB) method (Murray and Thompson, 1980). DNA sequencing with Applied Biosystems BigDye Terminator Cycle Sequencing was performed according to manufacturer's instructions by the Hubbard Center for Genome Studies (University of New Hampshire, Durham, NH). TOPO cloning was performed with fresh PCR products and vector pCR2.1-TOPO, according to manufacturer's instructions (Invitrogen, Carlsbad, CA). Transformation of chemically competent *E. coli* TOP10 was performed according to manufacturer's instruction. Transformants were cultured on LB agar containing appropriate antibiotics at 37°C.

Genus verification

Transposon mutants were verified to be *Photorhabdus* by 16S PCR of gDNA with primers 27F and 1492R as seen in Table 2 (Lane, 1991). Restriction Fragment Length Polymorphism was performed on PCR products with restriction enzyme *HaeIII* according to manufacturer's instructions (New England Biolabs). Digests were run on a 2% agarose gel in 1X TAE (40 mM Tris-acetate, 1 mM EDTA, pH 8.1-8.5) and fragment sizes were compared to that of the parental wild-type.

Table 2. Primers used in this study.

Primer	Primer set (5' to 3')	Gene	Reference
27F	F AGA GTT TGA TCA TGG CTC AG	Universal 16S rRNA	Lane, 1991
1492R	R ACG GCT ACC TTG TTA CGA CTT	Universal 16S rRNA	Lane, 1991
Ptemp02242	F TGA CTC GCC AGG GTG TCA AGA AAT R TGG CTG ACT ATG ATG TGG TGC TGA	<i>pte2242</i>	This study This study
Ptemp02243	F GGG ATC GGC CAA CAG TAT ATA GCA R CTT GCG ATC GTG TGG TGC AAT TCT	<i>pte2243</i>	This study This study
Ptemp02244	F TCT CTG CCA CCA GAA TCA CCA TGA R TTA GGG CCC GAA CCG TAA TGT CTT	<i>pte2244</i>	This study This study
Ptemp02245	F ACT GCT GGC TTG CTG AGT ACC ATA R ACG TTG TCT GCG TTT GAA GGA TGG	<i>pte2245</i>	This study This study
Ptemp02246	F CGT CAA GCC ATC ACT ACT CAG ACA R TGT GTT GTG CTC CTG TAG ACA GTT	<i>pte2245</i>	This study This study
64D5All	F CGT TTG CGC CAC CAA ATC ATC CA R ATT CGC TTG GAT GGC GTT ATC CCT	<i>pte2245</i> to <i>pte2246</i> in UNH6441	This study This study
1307	F CAG CCG TTA CGC TGT AGT TTG A R GTT GCT TGC TCG ACA CTG CTG ATT	External set of <i>pte2811</i> including operon	This study This study
Ptemp02811	F CAA TCC GCT GCT TGC ACA GCT AAA R ATT GTT GTT CCG TTC CTG CAT GGG	Internal set of <i>pte2811</i>	This study This study

Table 2 Continued

M13 R (-40 to -60)	TCA CAC AGG AAA CAG CTA TGA C		Michaels, 2006
M13 R (-27)	GGA AAC AGC TAT GAC CAT G	mini-Tn5	Michaels, 2006
Arb 1	GGC CAG GCG TCG ACT AGT ACN		
Arb 2	NNN NNN NNN GAT AT GGC CAC GCG TCG ACT AGT AC	Arbitrary primer	O'toole, 1999 O'toole, 1999
M13 F (-40 to -60)	CGC CAG GGT TTT CCC AGT CAC GAC		Michaels, 2006
M13 F (-20)	GTA AAA CGA CGG CCA GTG	mini-Tn5	Michaels, 2006
Kan	F GTA AAC TGG ATG GCT TTC TTG CCG R ATA TCA CGG GTA GCC AAC GCT ATG	Kanamycin resistance gene of pUB394	Michaels, 2006 Michaels, 2006

Southern Hybridization

Southern hybridization experiments were performed with a DIG High Prime DNA Labeling and Detection Starter Kit II (Roche Applied Science, Mannheim, Germany) under high stringency conditions using a modification of Southern (1975). PCR DIG probe synthesis was prepared previously (Michaels, 2006). The original vector, pUB394, as the template, the Kanamycin resistance gene of the mini-Tn5 insertion was amplified with the Kan primer set and purified (Table 2). The probe for the mini-Tn5 insertion was random primer labeled dioxigenin-11-dUTP with 1 μ g DNA according to manufacturer's instructions. Genomic DNA (10 μ g) and pUB394 (100 ng) were digested with restriction enzyme *NsiI* or *BglII* and separated by electrophoresis on a 0.8% agarose gel in 1X TAE (40 mM Tris-acetate, 1 mM EDTA, pH 8.1-8.5) at 6V/cm. The gel was soaked for 15 min in 0.25 N HCl with gentle agitation and washed with distilled water. After a 30 min incubation in 0.5 M NaOH and 1.5 M NaCl, the gel was washed and neutralized in 0.5 M Tris-Cl, pH 7.0, 3 M NaCl for 30 min. The gel was equilibrated in 20X SSC (3 M NaCl, 0.3 M sodium citrate, pH 7.0) for 5 min. A positively charged nylon membrane (Roche) was wetted in distilled water and soaked in 20X SSC. Gel and membrane were assembled into a reservoir transfer system with 20X SSC and DNA was transferred overnight by capillary action. The membrane was rinsed briefly in 2X SSC and baked for 2 h at 80°C in a glass dish. The membrane was prehybridized in preheated DIG Easy Hyb for 30 min at 42°C. For hybridization, 160 ng of DIG labeled probe was denatured at 100°C for 5 min and added to the membrane for an overnight

hybridization at 42°C. The membrane was washed twice at room temperature in 2X SSC and 0.1% SDS, for 5 min each with gentle agitation. At 67°C, the membrane was washed twice with preheated 0.5X SSC and 0.1% SDS for 15 min each with agitation. The membrane was rinsed in Washing buffer (0.1 M Maleic acid, 0.15 M NaCl, pH7.5; 0.3% Tween 20) for 5 min at room temperature. At 40°C, the membrane was incubated in 100 ml Blocking solution [in Maleic acid buffer (0.1 M Maleic acid, 0.15 M NaCl, pH 7.5)] for 30 min followed by a 30 min incubation in Antibody solution (1:10000 in Blocking solution). The membrane was washed twice in 100 ml washing buffer at 40°C. For equilibration, the membrane was soaked in 20 ml Detection buffer (0.1 M Tris-HCl, 0.1 M NaCl, pH 9.5) for 5 min. The membrane was placed DNA side up in a hybridization bag and 1 ml of CSPD ready-to-use was applied evenly to the surface. After a 5 min incubation at room temperature, excess CSPD was removed and the hybridization bag was sealed. The bag was allowed to incubate for 10 min at 37°C before exposing to X-ray film.

Arbitrary PCR

A modified arbitrary-primed PCR protocol was performed to amplify the DNA regions flanking the mini-Tn5 insertion (Caetano-Annoles, 1993; O'toole et al, 1999). The first round of arbitrary PCR was performed using primers M13R (-40 to -60) or M13F (-40 to -60) and Arb1 (see Table 2) from Integrated DNA Technologies, Inc. (Coralville, IA). First round thermal cycling (PTC-200, MJ Research, Waltham, MA) consisted of 95°C for 5 min; 6 cycles of 94°C for 30 sec,

30°C for 30 sec, 72°C for 60 sec; 30 cycles of 94°C for 30 sec, 45°C for 30 sec, 72°C for 60 sec, and a 5 min elongation at 72°C. Products were purified with QIAspin PCR Purification kit and eluted in 30 µl. A volume of 2 µl of this product was used for template of the second round of arbitrary PCR using primers M13R (-27) or M13F (-20) and Arb2. Second round (nested) thermal cycling included 30 cycles of 94°C for 30 sec, 45°C for 30 sec, 72°C for 60 sec; and a 5 min elongation at 72°C. Amplified products were electrophoresed in a 1% agarose gel with 1X TAE (40 mM Tris-acetate, 1 mM EDTA, pH 8.1-8.5) buffer. Second round product was purified and directly sequenced using either M13R (-27) or M13F (-20).

Gene Sequencing

The sequence of DNA flanking the mini-Tn5 was obtained by using M13F (-20) or M13R (-27) for arbitrary PCR product. DNA sequencing with Applied Biosystems BigDye Terminator Cycle Sequencing was performed according to manufacturer's instructions by the Hubbard Center for Genome Studies (University of New Hampshire, Durham, NH). The DNA sequences were analyzed by the use of the BioEdit program (Ibis Biosciences, Carlsbad, CA) and aligned to the *P. temperata* NC19 draft genome sequence. These data were also compared to the NCBI database using the BLAST program (<http://www.ncbi.nlm.nih.gov/BLAST/>) and/or the *Photorhabdus luminescens* TT01 genome database available at <http://genolist.pasteur.fr/PhotoList/>.

P. temperata NC19 Genome Draft Sequence

The *P. temperata* NC19 genome was sequenced by 454 pyrosequencing at Indiana University. Both a standard platform and pair-end sequencing were performed and the reads were assembled into 17 scaffolds.

Confirmation of Gene Identification

To confirm the presence of the transposon within a gene found by arbitrary PCR sequencing results, primers were designed from the draft genome sequence (Integrated DNA Technologies, Coralville, IA). PCR with specified primers (Table 2) was performed on mutant and wild-type genomic DNA. Thermal cycling conditions consisted of 94°C for 5 min; 30 cycles of 94°C for 30 sec, 58°C for 30 sec, 72°C for 5 min; and a 7 min elongation at 72°C. Product size was compared to the wild-type by agarose gel electrophoresis. A mutant exhibiting a larger band than that of the wild-type indicated the presence of the transposon.

RNA extraction and DNase treatment

Overnight cultures were subcultured in LB medium and grown to an OD₆₀₀ of ~0.7 before harvesting by centrifugation at 10,000 x g for 10 min. Pellets were frozen and stored at -80°C until RNA extraction. Thawed pellets were resuspended in 100 µl lysis solution [1 mg/ml lysozyme in 0.1% DEPC (diethyl pyrocarbonate) treated TE Buffer (1mM EDTA, 10 mM Tris)] and incubated for 10 min at room temperature. The RNA was extracted by the use of the Qiagen RNAeasy Mini Kit (Qiagen Sciences, Valencia, CA) and the manufacturer's protocol was followed except for the final elution step: 50 µl of nuclease-free water was added directly to the column membrane and incubated at room temperature for 10 min before elution. To remove residual DNA, RNA samples

were treated with RNase-free DNase as follows: 50 μ l RNA, 10 μ l 10X DNase I buffer (New England Biolabs, Ipswich, MA), 5 U DNase I (2U/ μ l; New England Biolabs, Ipswich, MA), 5 μ l RNase Out recombinant ribonuclease inhibitor (40 U/ μ l; Invitrogen, Carlsbad, CA) and RNase-free water to reach a total reaction volume of 100 μ l. Samples were incubated at 37°C for 30 min. DNase activity was inactivated with the addition of 1 μ l 0.5 M EDTA pH 8.0 (Ambion, Inc, Austin, TX) and a 10-min incubation at 75°C. RNA yield and purity (260 nm/280 nm ratio of ~ 2.0) was determined by a NanoDrop 1000 spectrophotometer (Thermo Scientific, Wilmington, DE). Following RNA quantification, the RNA samples were stored at -80°C until cDNA synthesis.

RT-PCR and cDNA synthesis

Gene expression was determined by RT-PCR. cDNA synthesis was performed with random hexamers by the use of a qScript cDNA synthesis kit (Quanta Biosciences, Gathersburg, MD) according to the manufacturer's instructions with approximately 300 ng RNA. Thermal cycling parameters consisted of 22°C for 5 min, 42°C for 30 min, and 85°C for 5 min. cDNA yield and purity was determined by a NanoDrop 1000 spectrophotometer. End-point PCR amplification with specific primers (Table 2) and approximately 500 ng of cDNA template was used to identify mRNA expression. Thermal cycling parameters included 94°C for 5 min; 30 cycles of 94°C for 30 sec, 57°C for 30 sec, 72°C for 90 s; and a 7 min elongation at 72°C. PCR amplicons were visualized by agarose gel electrophoresis.

Genetic Complementation

Wild-type genes were first cloned by the use of a TA TOPO cloning kit according to manufacturer's instructions (Invitrogen). Genes of interest were PCR-amplified with 150 ng parental wild-type gDNA as template and designed primers (Table 2) as described previously. External primers were specifically used for this study (Figure 2). Fresh PCR products were ligated into the TOPO cloning vector and transformed into *E. coli* TOP10 cells. Colonies containing the cloned genes were identified on LB plates containing Kanamycin and X-gal (20 mg/ml). Positive colonies were picked and inoculated into broth medium. Plasmid isolations were performed on cultures after an overnight incubation at 37°C. The restriction patterns for the plasmids were evaluated for restriction sites with SeqBuilder software (DNASTar, Inc., Madison, WI). The purified plasmids were digested with *Apa*I (*pte*2245) or *Eco*RV (*pte*2811) and the fragments were sized by agarose gel electrophoresis analysis. Insert orientation was determined with restriction digests and confirmed by sequencing with the primer M13F (-20). The TOPO clone and the expression vector, pBAD18-Cm (Guzman et al, 1995), were cut with restriction enzymes, *Hind*III and *Xba*I according to manufacturer's instructions (New England Biolabs). These specific enzymes enable the TOPO insert to be subcloned into the expression vector in the forward orientation. The expression vector was treated with Calf Intestinal alkaline phosphatase (New England Biolabs) to dephosphorylate the ends of the vector and prevent self-ligation. Manufacturer's instructions were followed except that 1 U (1 U/ l) was added directly to the 20 l restriction digest and the reaction mixture was incubated at 37°C for 30 min. Sample purification was performed with Qiagen PCR Purification kit to remove bound CIP. For ligation,

the insert was added to the vector in a 5:1 insert to vector ratio using 400 U of T4 ligase (New England Biolabs). The mixture was incubated at room temperature overnight. The construct (4 μ l) was added to 50 μ l electrocompetent *E. coli* DH5 and transferred to a chilled 0.2 mm cuvette. The vector was introduced into the cells by electrotransformation by the use of an electroporator (*E. coli* Pulser, BIO-RAD, Hercules, CA) at 12500 V/cm and 200 μ s. Immediately after electroporation, 500 μ l SOC medium (2% Bacto-tryptone, 0.5% yeast extract, 0.058% NaCl, 0.019% KCl, 0.2% MgCl₂-6H₂O, 0.49% MgSO₄-7 H₂O, 0.36% Glucose) was added to the cuvette and transferred to a fresh tube. Bacterial suspensions were incubated at 37°C with gentle shaking for 1 h. Transformants were cultured on LB plates supplemented with chloramphenicol (25 μ g/ml) at 37°C overnight. Potential transformants were isolated and retained for further use. To confirm the transformants, the plasmids were purified, digested with *Sfi*I to linearize the plasmid, and electrophoresed on a 1% agarose gel in 1X TAE (40 mM Tris-acetate, 1 mM EDTA, pH 8.1-8.5) to confirm identity. The confirmed plasmids were electroporated into the parental wild-type of *P. temperata* NC19 as described above, however, electroporation recovery and selection incubation was performed at 28°C. Transformants were confirmed as described above. Due to difficulties directly transforming the mutant cells, the construct was first introduced into *P. temperata* wild-type cells. The purified construct from the wild-type cells was used for the electrotransformation experiments with the mutants.

Expression of Complemented Mutants

To examine expression of complemented mutants, phenotypic assays were performed as described above, with the addition of 0.2% arabinose to all media.

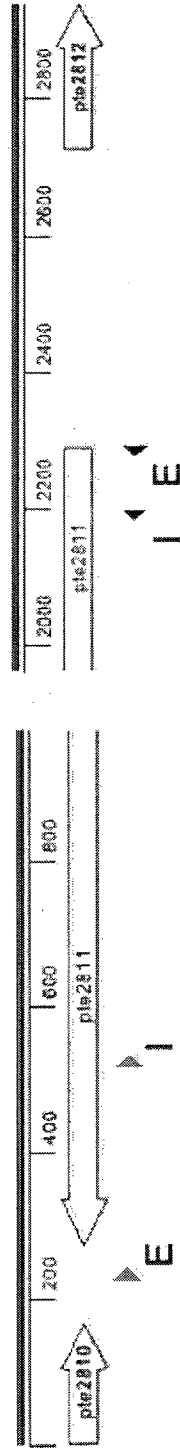


Figure 2. The amplification of *pte2811*. External primer set (E), 1307F/R, was used for cloning. Internal primer set (I), ptemp2811F/R, was used for expression.

CHAPTER III

RESULTS

Identification of Pathogenesis Mutants

A *Photorhabdus temperata* mutant library consisting of approximately 10,000 transposon mutants was previously generated and screened for altered motility by swim and swarm plate migration assays (Michaels, 2006). A total of 86 mutants were identified and categorized into 5 phenotypic groups: hyperswarmers (33), hyperswimmers (12), nonmotiles (23), defective/aberrant swimming (12), and mutants capable of swimming without salt (6). This mutant library was also screened for the ability of binding calcofluor-white, a whitening agent found in bleach (Gately and Tisa, unpublished). Secondary phase cells bind the calcofluor, while the primary phase cells do not bind it. The purpose of this study was to identify motility mutants with altered virulence. All 86 motility mutants and 11 primary phase calcofluor-binding mutants were screened for altered pathogenesis properties by use of the *in vivo* wax moth test system. Approximately 100 cells were directly injected into the host-insect *G. mellonella*, and mortality over time was determined (Figure 3). The parental wild-type primary phase cells killed all of the larva injected by 46 h (LT_{100}) and required 38 h to kill 50% of the population (LT_{50}). From the first screen with a 100 cell dose, 14 of the 96 mutants tested exhibited faster or slower LT_{50} and LT_{100}

values than the parental wild-type. These mutants included the following categories: 4 hyperswarmer mutants (UNH1201, UNH5006, UNH8309, and UNH8322); 3 hyperswimmer mutants, (UNH6290, UNH7504, and UNH9304); 3 nonmotiles (UNH427, UNH2072 and UNH8678); 3 motility-defective mutants (UNH1307, UNH5832 and UNH6441); and 1 calcofluor-white-binding mutant (UNH2033). Of these 14 mutants, 5 mutants (UNH5832, UNH2072, UNH9304, UNH8322, and UNH6290) had lower LT_{50} and LT_{100} values, which suggested enhanced virulence. There were 9 mutants (UNH1307, UNH6441, UNH2033, UNH427, UNH8309, UNH7504, UNH1201, UNH5006, and UNH8678) with elevated LT_{50} and LT_{100} values implying reduced virulence. All of the mutants killed the insects over time. No mutants were identified that were completely defective in pathogenesis. These 14 mutants were selected for further study.

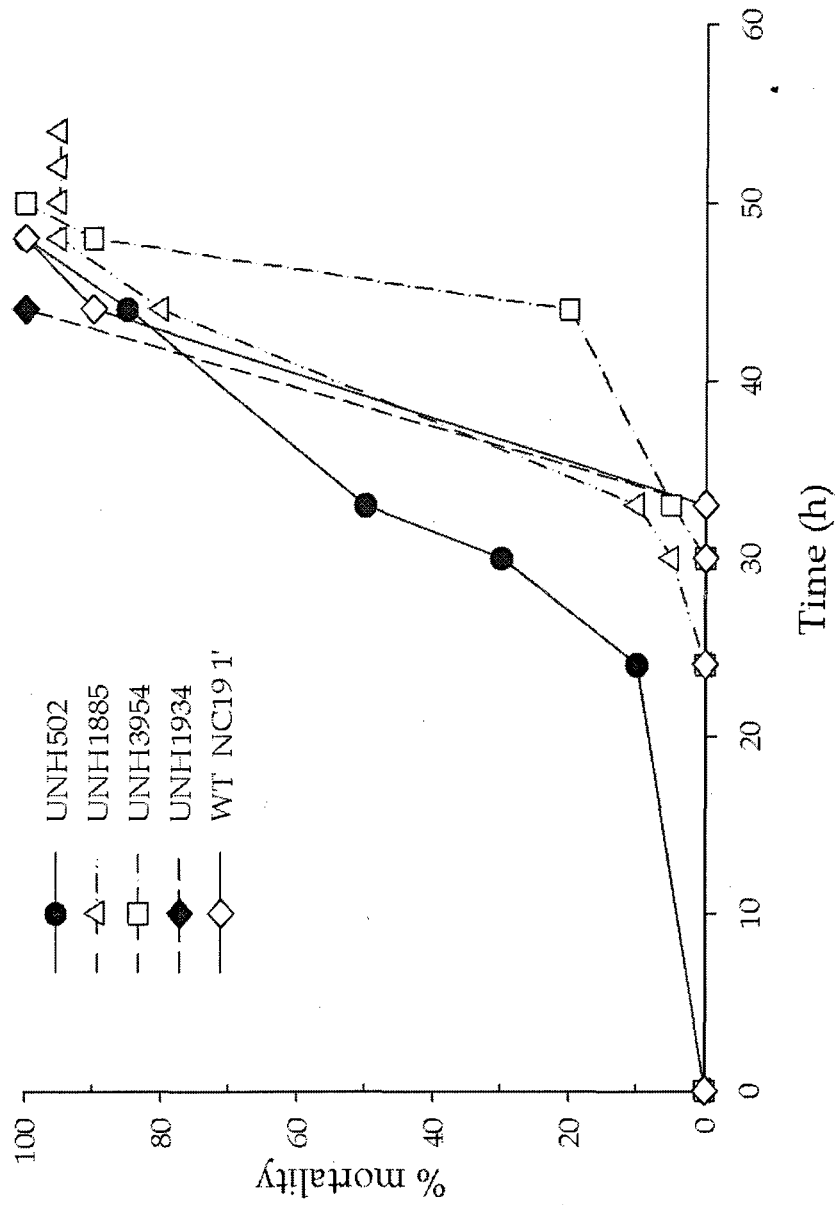


Figure 3. *In vivo* insect pathogenesis assays revealed mutants with reduced and enhanced insect virulence. Lethal time was determined for each mutant injecting 20 *G. mellonella* larvae. The LT_{50} value was defined as the time required for 50% of the larvae to die, while LT_{100} value was defined as the time required for 100% mortality in this screen.

Confirmation of Pathogenesis Mutants

All of the above identified 14 mutants with altered virulence were confirmed to be *Photorhabdus* mutants and not contaminants by the use of Random Fragment Length Polymorphism and sequencing of the 16S RNA. One possible explanation for these differences in virulence levels could be attributed to variation in viable cell numbers. To verify these changes in virulence, the effect of dosage was tested. The larvae were directly injected with dosages ranging from 10 to 10000 cells per insect. The objective of these experiments was to identify those mutants that consistently caused an altered mortality rate at each dosage. A dose-dependent response was observed for both LT_{50} and LT_{100} determinations (Figure 4). While 10 mutants showed similar virulence to the parental wild-type, four mutants maintained an altered virulence pattern over the range tested. This group was comprised of 3 defective-motility mutants (UNH1307, UNH5832, and UNH6441) and one calcofluor-binding mutant (UNH2033). UNH5832 exhibited enhanced virulence, causing mortality at a rate of approximately 10 h faster than the parental wild-type. The other 3 mutants, UNH1307, UNH2033, and UNH6441, exhibited a delayed pathogenesis response and killed larva at approximately 10-20 h slower rate than the parental wild-type. These rates of mortality were consistent for both LT_{50} (Figure 4A) and LT_{100} (Figure 4B) values. These four mutants were further examined at the genetic and physiological levels. The remaining 10 mutants were saved for phenotypic characterizations and will be re-examined for pathogenicity at a later date.

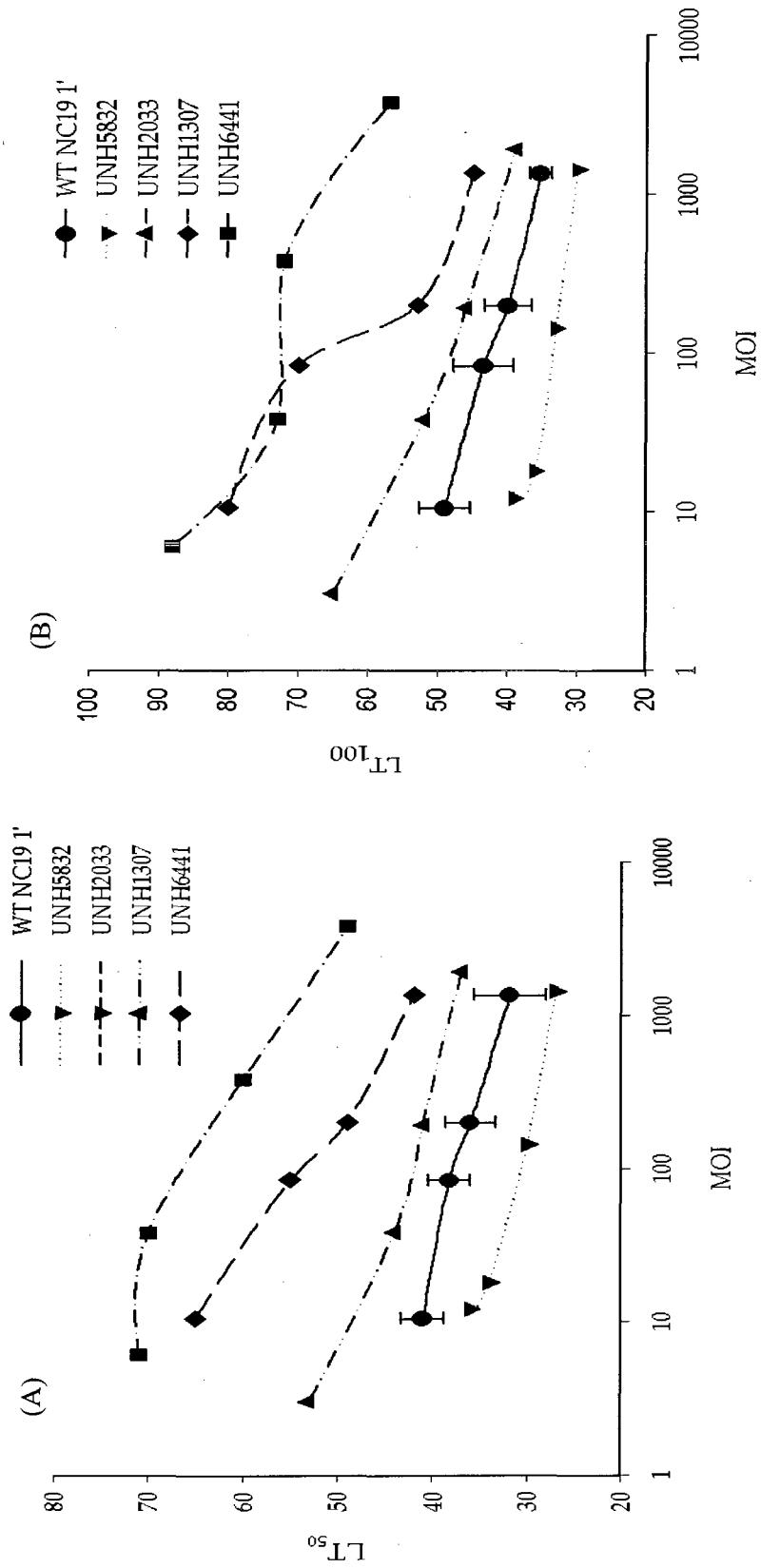


Figure 4. Verification of mutants exhibiting altered virulence. (A) The effect of dosage or multiplicity of infection (MOI) on LT₅₀ values and (B) the effect of MOI on the LT₁₀₀ values. From this study, mutants UNH6441, UNH2033 and UNH1307 were determined to have delayed pathogenesis response while mutant UNH5832 exhibited enhanced response.

Identification of Symbiosis Mutants

Besides pathogenesis, another important aspect of the *Photorhabdus* lifecycle is the symbiosis with a nematode host. Although not the major focus of this study, symbiosis was examined to see a potential overlap of mutants defective in both aspects of the lifecycle. Motility mutants used above in the pathogenesis screens were examined for their ability to support the growth and development of *H. bacteriophora* nematodes. All 86 motility mutants and 11 calcofluor mutants were screened for symbiosis defects or changes via a nematode plate assay described in the methods. Cultures capable of supporting nematode growth were clearly identified by a white mass of nematodes (Figure 5). Capabilities were compared to two positive wild-type controls, *P. temperata* strains NC19 1° and Meg1. Negative controls included *P. temperata* NC19 2°, *E. coli*, and sterile lipid agar. Although the majority of the mutants had wild-type symbiosis capabilities, a few mutants were identified that had altered symbiosis capabilities. From the initial screening, 2 mutants (UNH8776 and UNH8178) appeared to be completely defective in symbiosis. Two mutants (UNH5832 and UNH1201) had an accelerated rate of symbiosis formation that resulted in a mature mass of IJs a few days earlier than the parental wild-type. Two mutants (UNH6427 and UNH8191) showed delayed symbiosis response forming a nematode mass a few days later than wild-type. Since all 6 mutants and the wild-type cells had the same growth rate, these differences in symbiosis were not correlated to growth rate. This group of symbiosis mutants included 3 hyperswarmer mutants (UNH1201, UNH8191, and UNH8178) and 3 motility-defective mutants (UNH5832, UNH6427, and UNH8776).

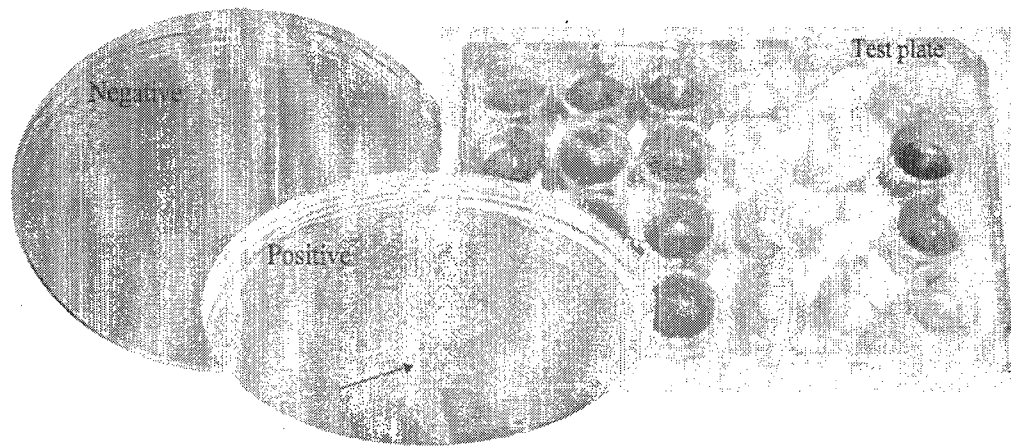


Figure 5. Mutants were screened for symbiosis in a 24-well test plate containing lipid agar. Plates were incubated at room temperature for 21 d. A strain testing positive formed a white mass of aggregated adult nematodes.

Confirmation of Symbiosis Mutants

Six putative symbiosis mutants were confirmed as *Photorhabdus* by 16S PCR and RFLP analyses and were not contaminants. To confirm results found in the initial symbiosis screen, the assay was repeated on individual lipid agar plates, rather than a 24-well plate. This 2nd round verification step reduced the above number to two mutants, both defective in motility and altered in symbiosis capabilities. UNH6441 exhibited a delayed-symbiosis trait that showed nematode development occurring approximately 2 days later than the parental wild-type. UNH5832 showed an accelerated-symbiosis trait that resulted in nematode development approximately 2 days earlier than the parental wild-type. Both of these mutants were also altered in their insect pathogenesis response. UNH5832 showed both accelerated nematode development and enhanced virulence. Initial pathogenesis screening indicated that UNH6427 showed both a delayed pathogenesis response and symbiosis capabilities. For an overall understanding of these mutant phenotypes, several physiological assays were completed on them as described below. The remaining 4 mutants were stored and will be re-examined for symbiosis defects at a later date.

Phenotypic Characterization of Pathogenesis and Symbiosis Mutants

Several phenotypic properties of the pathogenesis and/or symbiosis mutants and their parental wild-type were investigated (Table 3). The results of the 5 mutants were compared to the parental primary and secondary phase wild-type cells. The parental primary wild-type cells bind dyes on MacConkey and

EMB media, and two mutants (UNH6441, UNH5832) retained this dye-binding ability. Three mutants (UNH1307, UNH6441, and UNH2033) did not bind dye, which is similar to the secondary phase wild-type trait. However, all of these 3 mutants retained the ability to form a symbiosis with nematodes, which is a primary phase trait. Secondary phase cells will not support nematode growth or development. Colony morphology and pigmentation on LB agar plates differed for these mutants. Primary phase parental wild-type produced yellow colonies on LB, but mutants UNH1307 and UNH2033 formed white colonies, similar to secondary phase cells. The ability to bind the whitening agent, calcofluor-white, was re-evaluated with interesting mutants. UNH2033, similar to the secondary phase wild-type is capable of binding this agent. Previous studies have shown that this may indicate an altered cell surface (Janicki and Tisa, unpublished).

Several extracellular activities were tested. All of the mutants had lipase activity, while DNase and protease activities varied. UNH1307 was defective for both DNase and protease activity, while UNH6427 was defective in DNase activity. Wild-type primary phase cells exhibit annular hemolysis on blood agar plates (BAP) that is characteristic for this bacterium. Three mutants with delayed pathogenesis (UNH1307, UNH6441, UNH6427) were deficient in hemolysis activity. However, UNH5832, which exhibited enhanced virulence, produced a larger zone of annular hemolysis than the parental wild-type.

Photorhabdus spp. are producers of antimicrobial activity (Waterfield et al, 2009) but is typically assayed with one indicator strain *Micrococcus luteus*. Other indicator strains, *Bacillus subtilis*, *Escherichia coli*, and *Staphylococcus aureus* were used in this study to examine a broader range of organisms. Antibiotic activity (AB Act) of all mutants was tested with the four indicator cultures (Figure 6). *P.*

temperata did not inhibit *E. coli* growth. Two mutants, UNH2033 and UNH1307, had no antibiotic activity against any of the indicator cultures. The remaining mutants tested inhibited the indicator strains at levels similar to the parental wild-type. Under these conditions, secondary phase cells do not produce antibiotic activity (Hodgson et al, 2003).

The growth rates for all of the mutants were determined over 24 h at 28°C. All mutants exhibited a growth rate similar to the parental primary phase wild-type cells (Data not shown). These data indicate that all of the changes observed in pathogenesis and symbiosis patterns were not growth related.

Table 3. Physiological characterization of selected transposon mutants

Mutant	Mortality		Symbiosis	Motility	Dye-Binding		DNase	Protease	BAP	AB Act
	LT ₅₀	LT ₁₀₀			Mac	EMB				
WT NC19 1°	38	46	+	WT	+	-	3	4	2	+
WT NC19 2°	35	43	-	WT	-	+	2	3	0	-
UNH1307	55	68	+	Defective	-	-	2	0	0	-
UNH2033	46	54	+	WT	-	+	2	2	1	-
UNH6441	66	72	+	Defective	+	-	3	4	1	+
UNH5832	32	35	Enhanced	Defective	+	-	3	4	2	+
UNH6427	52	58	Delayed	Defective	-	-	3	4	2	+

Symbiosis: (+) Capable of nematode development similar to WT; (-) Incapable of development; Enhanced: nematode development approximately 2 d faster than WT; Delayed: development 2 d slower. MacConkey(MAC): (+) absorbs dye; red; (-) clear. EMB: (+) absorbs dye; metallic green sheen; (-) purple. Calcofluor: (+) Binds Calcofluor; fluorescent; (-) no binding. DNase and Protease values indicate measurement of halo clearing around the colony (mm) after 48 h incubation; Blood agar plate (BAP); values indicate measurement of annular hemolysis around colony (mm) after 48 h incubation; Antibiotic Activity (AB Act): (+) zone of inhibition against indicator strains; (-) no zone of inhibition.

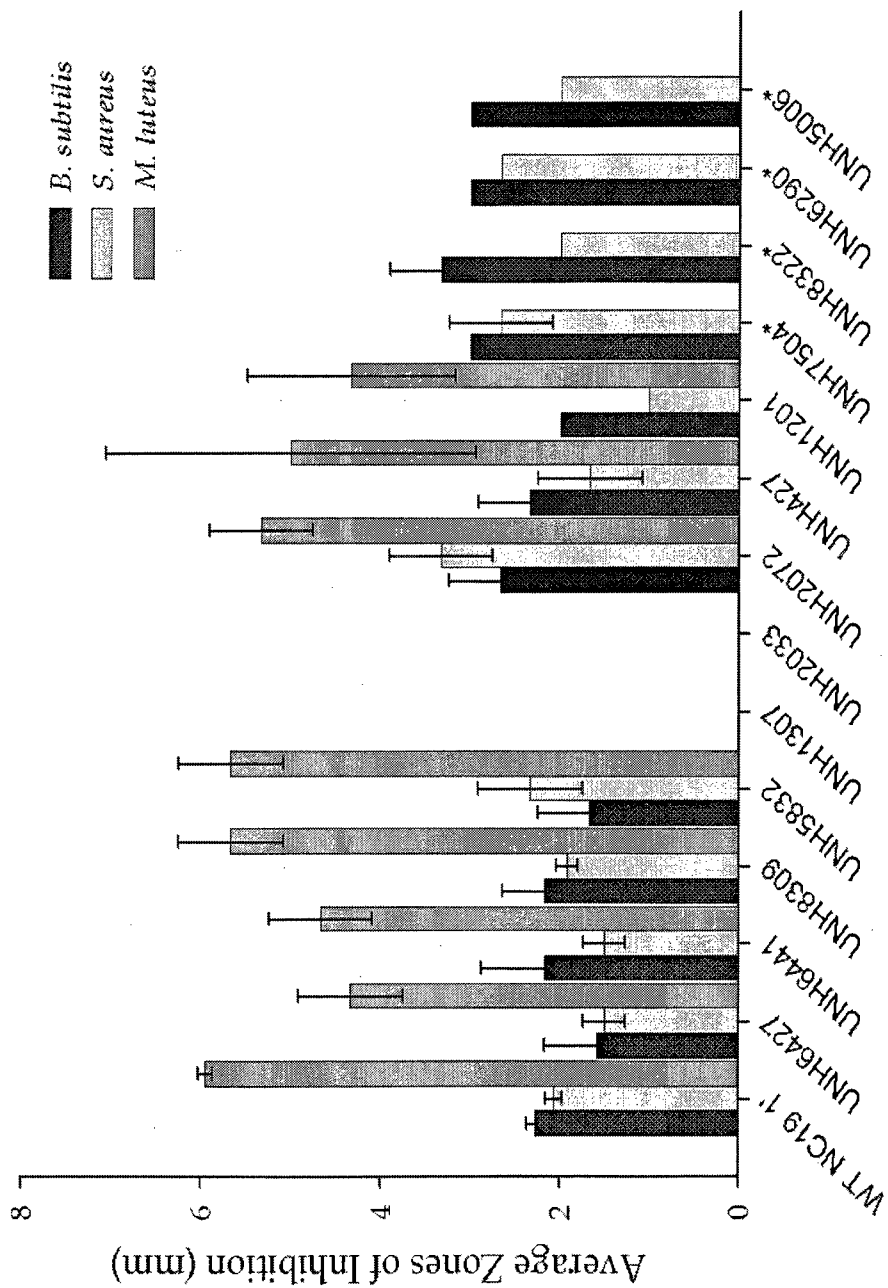


Figure 6. Antibiotic activity physiologically characterized interesting mutants. Average zones of inhibition were measured on indicator cultures. Note:* indicates no data for *M. luteus*.

Molecular characterization of Pathogenesis and Symbiosis mutants

The confirmed pool of mutants described above was further analyzed to identify the sites of the mutation. Southern analysis of the mutants verified random transposition of the mini-Tn5 transposon and the presence of a single insertion site for each mutant (Figure 7). However, the results for mutant UNH6441 were inconclusive and no bands were observed for either digestion.

Arbitrary PCR was utilized to identify the specific transposon-disrupted gene for each mutant. Though attempted on all confirmed mutants, this method was only successful in 3 mutants. Sequencing of arbitrary products determined gene disruptions in each mutant (Table 4). These experiments were facilitated by the generation of the sequenced *P. temperata* NC19 genome, which provide a better database to match sequence information. Sequencing results of UNH1307 identified a 100% match to the *pte2811* gene in the *P. temperata* genome. This gene had 91% (513/558) identity on a protein basis to *plu2384* of *P. luminescens* genome and was identified as RNase II by *in silico* analysis with NCBI BLAST program. UNH6441 and UNH6427 sequencing results identified *pte2245* with a 100% and 96% match, respectively, when compared to the *P. temperata* genome. *In silico* analysis of *pte2245* (98% (237/241) identity to *plu0425*) identified this gene as a hypothetical protein, which showed similarity to *yheO* of *E. coli*.

The site of the gene insertion was confirmed by a PCR approach. The identified genes were amplified by PCR with specific primers (Table 2) and amplicons were visualized by electrophoresis. Mutants with the insertion resulted in bands that were significantly larger than that of the wild-type control (Figure 8) which verified the presence of the transposon. These experiments

were followed by RT-PCR expression studies. RNA was extracted for each confirmed mutant and cDNA synthesis was performed with random hexamers. End-point RT-PCR with primer set ptemp02811 revealed *pte02811* gene was expressed in the parental wild-type, but not in mutant UNH1307. Analysis of UNH6441 and UNH6427 by end-point RT-PCR revealed that *pte2245* was the only gene to not be expressed. These results indicate the transposon caused a disruption of these genes and result in the given phenotypes.

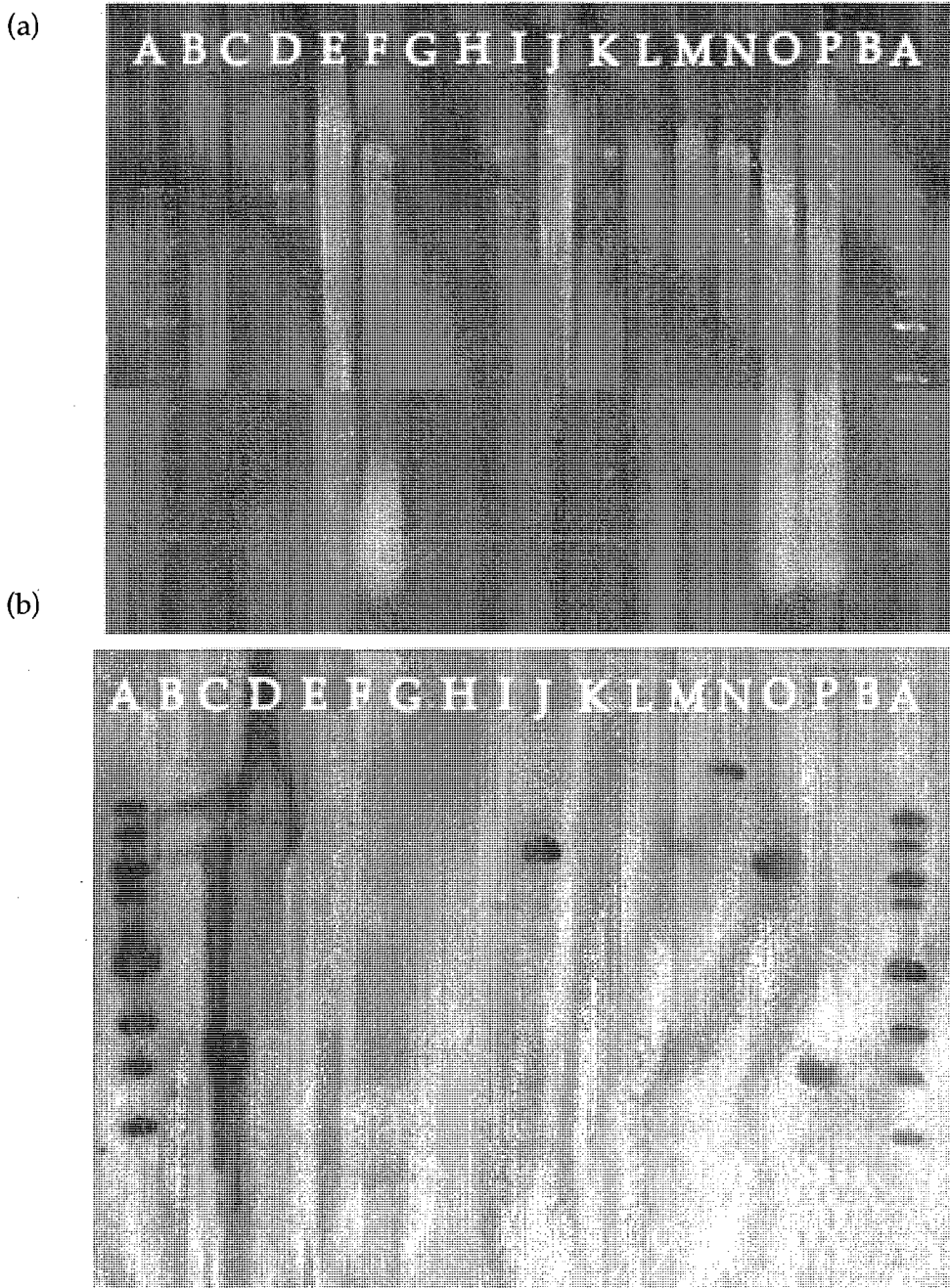


Figure 7. A single insertion of the mini-Tn5 transposon determined by a Southern hybridization. (a) Restriction digests of genomic DNA were separated via 0.8% agarose gel electrophoresis in TAE at 6V/cm. (b) A southern hybridization of capillary transferred DNA. A: 1Kb ladder; B: DIG ladder; C: pUB394 *Bgl*III; D: pUB394 *Nsi*I; E: 1' WT *Bgl*III; F: 1' WT *Nsi*I; G: UNH6441 *Bgl*III; H: UNH6441 *Nsi*I; I: UNH1307 *Bgl*III; J: UNH1307 *Nsi*I; K: UNH5832 *Bgl*III; L: UNH5832 *Nsi*I; M: UNH8309 *Bgl*III; N: UNH8309 *Nsi*I; O: UNH6427 *Bgl*III; P: UNH6427 *Nsi*I.

Table 4. Genetic identification of selected transposon mutants.

Mutant	% Identity	<i>pte</i>	<i>plu</i>	Identity
UNH6441	100 (129/129)	<i>pte2245</i>	<i>plu0425</i>	Unknown (<i>yheO</i>)
UNH6427	96 (125/129)	<i>pte2245</i>	<i>plu0425</i>	Unknown (<i>yheO</i>)
UNH1307	100 (574/574)	<i>pte2811</i>	<i>plu2384</i>	RNase II

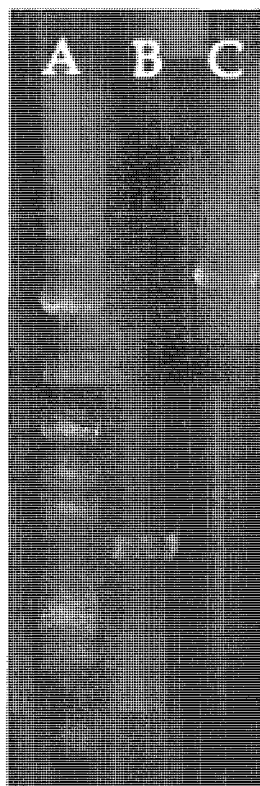


Figure 8. A PCR approach confirmed arbitrary PCR sequencing results. Specific primers for *pte2245* were used to amplify (A) the parental wild-type and (B) the mutant UNH6441 (B). A significant increase in mutant band size indicated the presence of the transposon. This was performed on all arbitrary sequencing results and compared to a 2-Log DNA ladder (New England Biolabs).

Genetic complementation of UNH1307

Although these transposon mutants showed these specific defects in pathogenesis and motility, the definitive link to demonstrate causality is genetic complementation. The 3 mutants with disruptions in *pte2811* (UNH1307) or *pte2245* (UNH6441, UNH6427) were chosen for these experiments and a PCR approach was taken. The wild-type *pte2811* gene was amplified using external primers (1307) and cloned into a TOPO vector. This construct was transformed into TOP10 cells, and positive colonies were selected and confirmed. The cloned gene was subcloned in the pBAD18-Cm expression vector as described in the methods. The resulting construct was an 8 Kb plasmid, pHR1 (Figure 9). This construct features chloramphenicol resistance for selection, and the complete *pte2811* gene under an arabinose-inducible promoter. After electroporation of pHR1 into *E. coli* DH5 α , chloramphenicol-resistant transformants containing pHR1 were isolated and the plasmid was confirmed by *SalI* restriction digest and gel electrophoresis. After several attempts, the pHR1 plasmid could not be introduced directly into UNH1307. Because of the difficulties of transforming directly into the mutant, pHR1 was first electrotransformed into the parental wild-type, NC19 1 $^{\circ}$ before introduction into the mutant strain. Control plasmid pBAD18-Cm was also introduced into the parental wild-type and the mutant strain. UNH1307 cells complemented with pHR1 were immediately recognized and had different appearance from the UNH1307 with the control vector. HNR1307 recovered pigment production activity, while control HNR1318 did not.

cDNA synthesis and end-point RT-PCR verified the expression of *pte2811* in the complemented mutant, HNR1307 (Figure 10). The physiological properties

of the UNH1307 mutant and complemented mutant were investigated (Table 5). Genetic complementation (HNR1307) restored UNH1307 to primary phase wild-type pattern for all of the traits tested. It was immediately noticed that the complemented mutant, HNR1307 returned to yellow pigmentation on LB agar plates. Dye-binding on MacConkey plates and hemolysis and DNase activity were restored to the wild-type levels. Over-expression of *pte2811* (HNR0606) caused more dye-binding on MacConkey plates and created more annular hemolysis on blood agar than the parental wild-type.

The UNH1307 mutant was originally identified as aberrant motility mutant (Micheals, 2006). Figure 11 shows the results of a swim-ring-migration assay. Genetic complementation of UNH1307 with the *pte2811* gene restored wild-type swimming. Surprisingly, the presence of arabinose had little effect of the swim formation (Figure 12). The control plasmid (HNR1318) did not complement the mutation. Both the control plasmid and the construction caused a slight increase in the swim ring diameter for the wild-type cells (HNR0018 and HNR0606). These data show causality for these physiological traits.

The key property for this study was insect pathogenesis. The UNH1307 mutant showed delayed insect pathogenesis. Figure 13 shows the results of an insect mortality assay. Genetic complementation (HNR1307) restored UNH1307 to wild-type virulence levels. Cells used in this assay were pregrown with arabinose to induce expression of *pte2811* gene. Wild-type cells over-expressing this gene were more virulent showing lower LT_{50} and LT_{100} values than the wild-type control. Uninduced complemented UNH1307 restored virulence but the LT_{50} and LT_{100} values did not reach the wild-type levels (data not shown).

As UNH1307 was also defective in antibiotic activity, antibiotic assays were completed with indicator strains. *P. temperata* cells were grown on PP3 medium supplemented with arabinose. Complementation only partially restored antibiotic activity (Figure 14). Though the complemented mutant inhibited the indicator cultures, the level of inhibition was less than the wild-type.

The construct, pHR1, was constructed with external primers of the wild-type gene, *pte2811* (Figure 2). This construct has a pBAD18-Cm backbone, and expression is tightly regulated by arabinose (Guzman et al, 2005). However, the presence of arabinose was not required for the expression *pte2811*. This was seen immediately by the restoration of pigment on LB agar plates upon transformation. The presence of arabinose also made little difference in the return of wild-type motility. These results indicate the cloning process created a promoter site within the pHR1 construct to allow expression without arabinose. The possible promoter region is indicated in Figure 9. *In silico* analysis does not determine a known promoter sequence within this region. It is possible that the *Photorhabdus* background caused a leaky arabinose promoter, constitutively expressing *pte2811*.

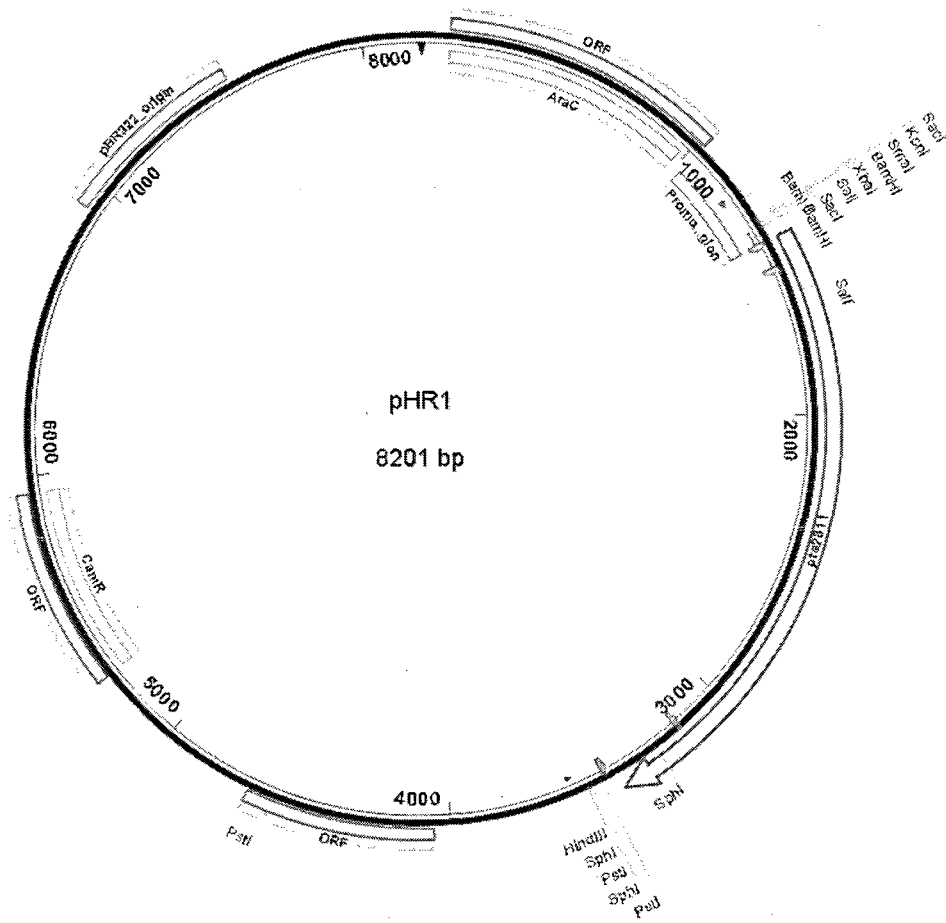


Figure 9. The pHR1 construct with a pBAD18 backbone. Indicated regions include chloramphenicol resistance, multiple cloning site, *pte2811* and the possible *pte2811* promoter region.

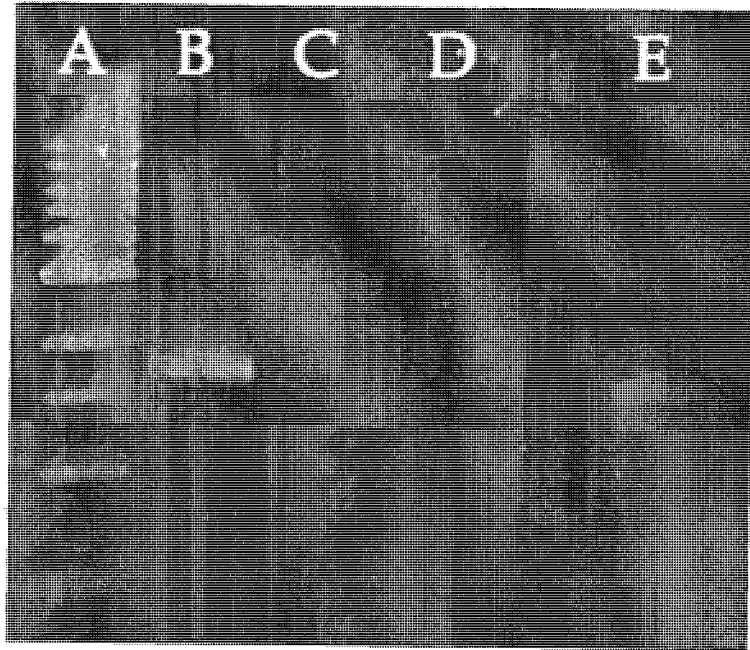


Figure 10. Genetic complementation and expression of *pte2811* was verified through cDNA synthesis and end-point RT-PCR. A: 1 Kb ladder; B: + WT gDNA; C: WT; D: UNH1307; E: HNR1307

Table 5. Genetic complementation of UNH1307 restores phenotypes

Mutant	Mortality		Motility	Dye-Binding		DNase	Lipase	Protease	BAP	AB Act
	LT ₅₀	LT ₁₀₀		Mac	Mac					
WT NC19 1°	38	46	WT	+	+	+	+	+	+	+
HNR0606	33	43	WT	+	+	+	+	+	++	+
UNH1307	60	72	Defective	-	-	-	-	-	-	-
HNR1307	47	53	WT	+	+	+	+	+	+	+

MacConkey (MAC): (+) absorbs dye; red; (-) clear. DNase: (+) Halo clearing around colony similar to WT; (-) no clearing.
 Lipase: (+) Halo clearing around colony similar to WT; (-) no clearing around colony. Protease (+) Halo clearing around colony similar to WT; (-) no clearing. Blood agar plate (BAP): (+) annular hemolysis; (-) no hemolysis (++) more annular (> 2 mm) hemolysis than WT. Antibiotic activity (AB Act): (+) zone of inhibition against indicator strains; (-) no zone of inhibition.

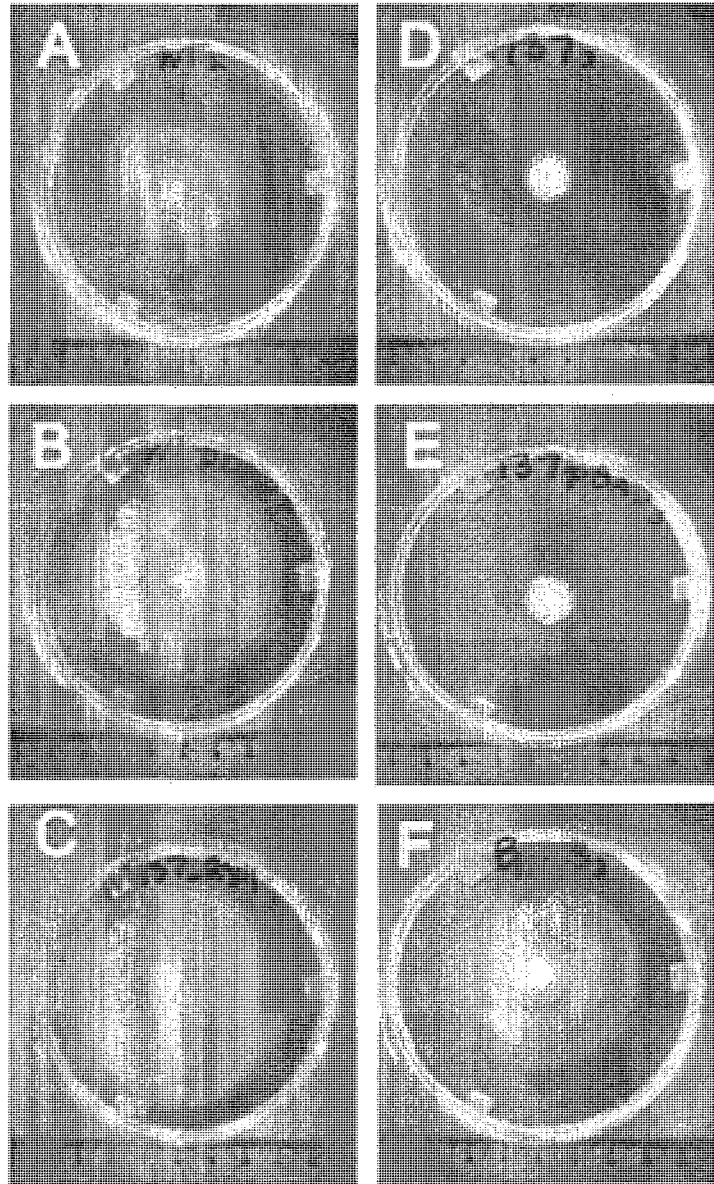


Figure 11. Genetic complementation restores swimming behavior in UNH1307. Swim migration plate assays were completed at 28°C for 48 h. Panels: (A) parental wild-type (B) HNR0018 (C) HNR0606 (D) UNH1307 (E) HNR1318 (F) HNR1307.

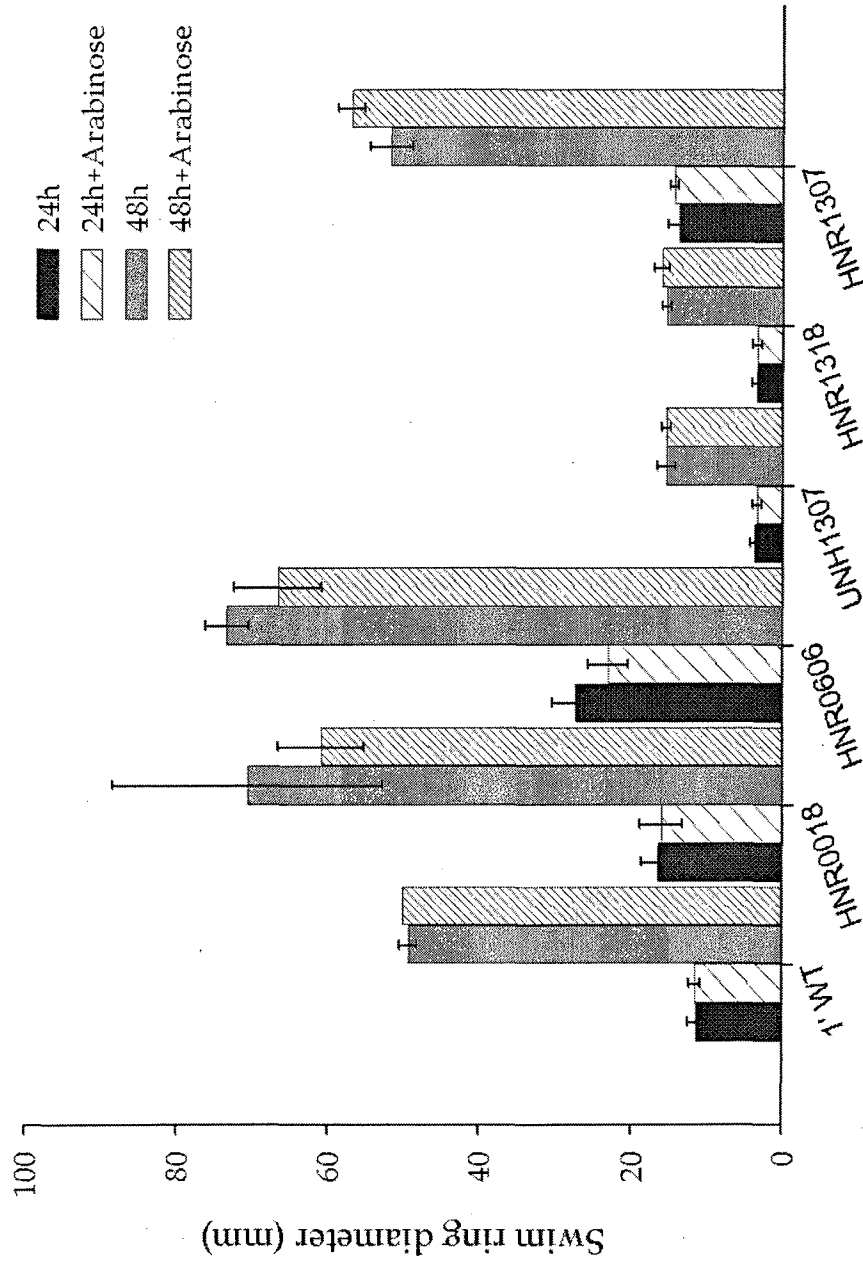


Figure 12. Arabinose was not required for restored swimming behavior for UNH1307. Swim migration assays were performed at 28° C over a period of 48 h, with and without the addition of

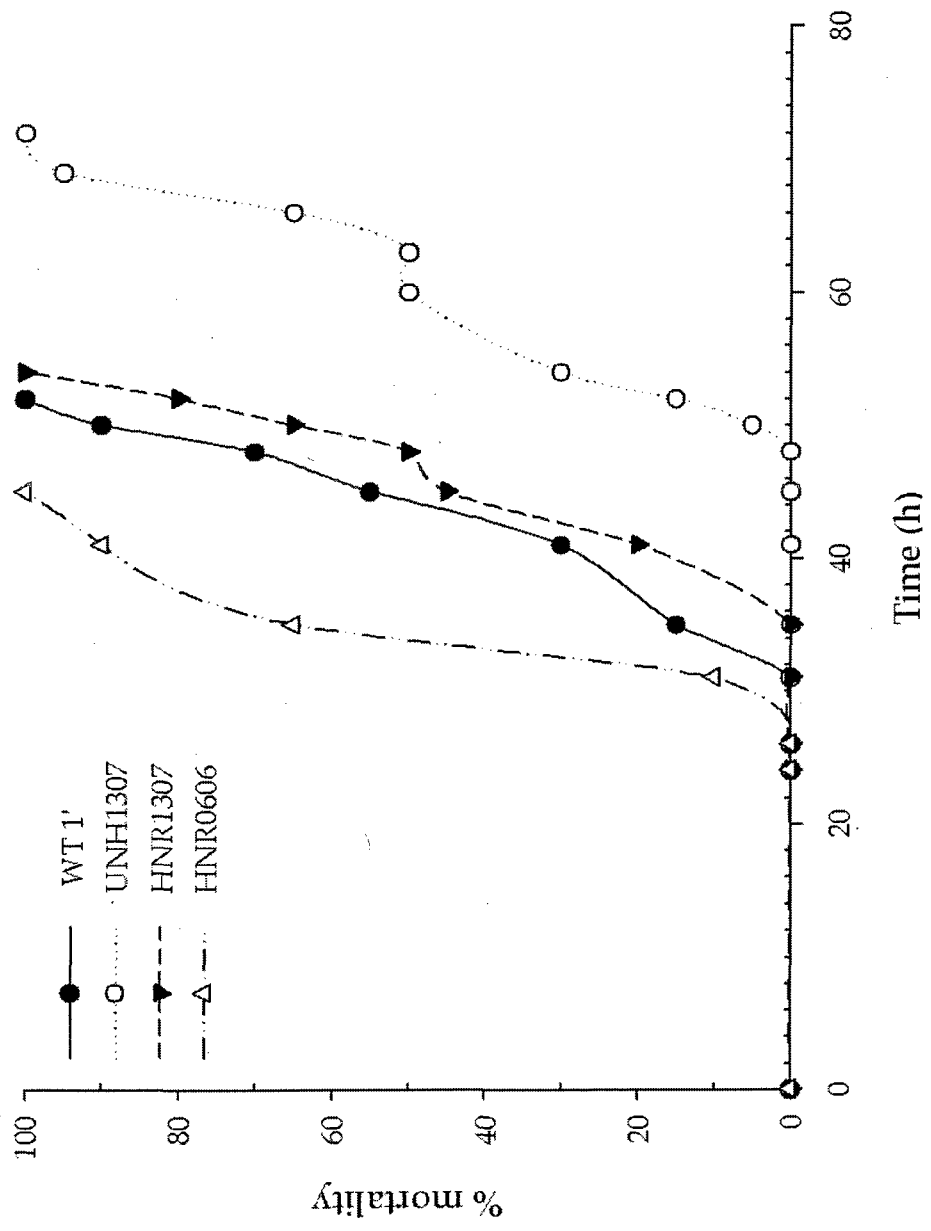


Figure 13. Genetic complementation restores virulence in UNH1307. Insect mortality was determined by the injection of *Galleria mellonella*. Media was supplemented with

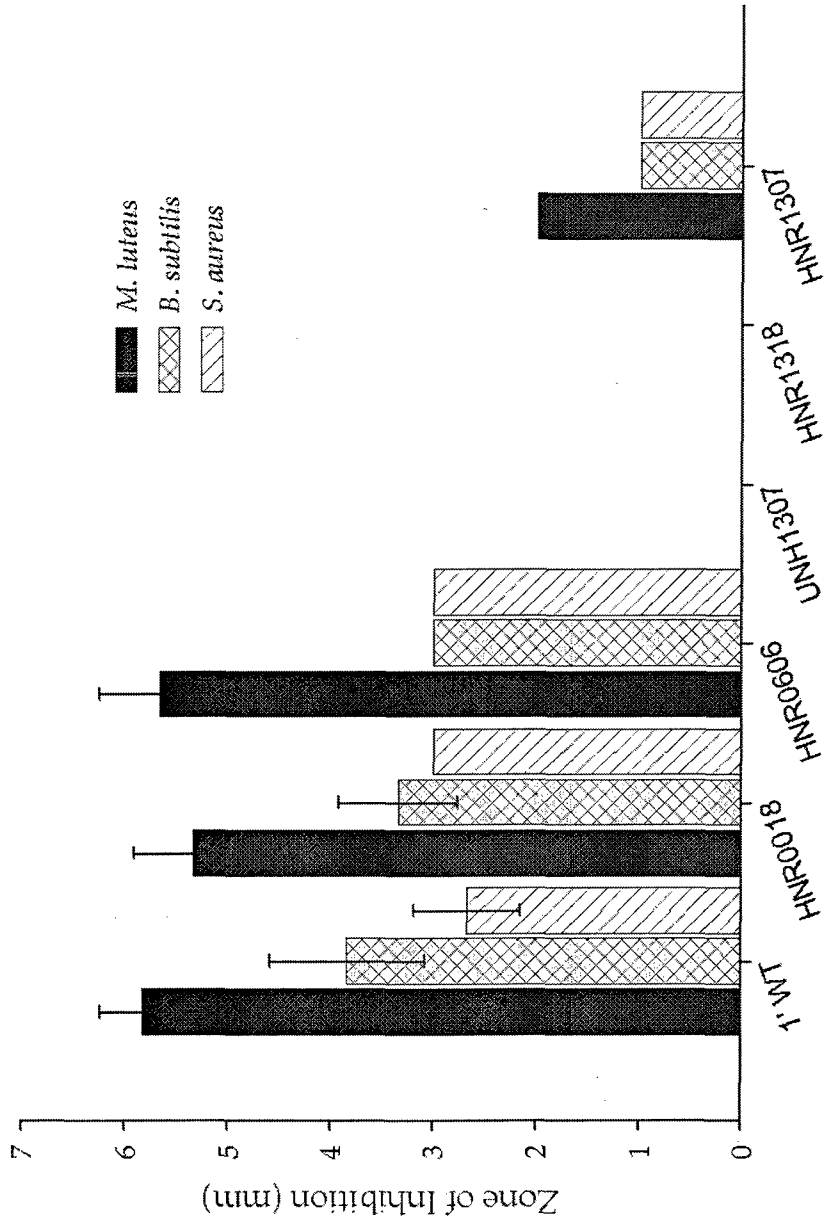


Figure 14. Genetic complementation of UNH1307 partially restores antibiotic activity. Confluent 72 h cultures were plated on indicator cultures at 37°C for 18 h.

CHAPTER IV

DISCUSSION

Use of Motility and Calcofluor-binding mutants for Pathogenesis Study

An initial screening of a transposon mutant library resulted in the identification of 86 motility mutants and 11 calcofluor-binding mutants (Michaels, 2006; Gately & Tisa, unpublished). This subset of mutants was chosen for the labor-intensive insect mortality screen and symbiosis screen based on physiological properties and the need to reduce the pool of candidates for these time-consuming assays. Given the environments *Photorhabdus* encounters, in addition to its ability to switch between pathogenic and symbiotic roles, motility is predicted to play an essential role in its life style. Although flagellar structural mutants indicate that motility is not required for the pathogenesis of *Photorhabdus*, motility does contribute to the competitive fitness during infection of both the insect and the nematode (Easom & Clarke, 2008). This competitive advantage is also true for other Enterobacteria such as *E. coli* or *Salmonella* spp. (Stetcher et al, 2008). With many pathogens, motility plays central roles in infection of the host cells, and the persistence of infection by adhering to host cell surfaces (Josenhans & Suerbaum, 2002). For example, in the mammalian pathogen, *Proteus mirabilis*, swarming behavior is essential for virulence as swarm-cell dependent proteins include virulence factors such as protease and

hemolysin (Schneider et al, 2002). Belas and Suvanasuthi (2005) linked *P. mirabilis* flagellum function and virulence expression to surface sensing. This indicates the expression of swarming behavior and virulence greatly depends on the surface infected. Syed et al (2009) showed motility is also required in the infection of the human intestinal tract for *Vibrio cholerae*, however, in this pathogen motility and virulence are inversely regulated. Motility is down-regulated as several virulence factors are simultaneously up-regulated once *V. cholerae* colonizes the intestinal cell surface. Based on the role of motility seen in other pathogens and the competitive advantage motility confers in *Photobacterium*, I hypothesized that highly motile mutants (hyperswarmers, hyperswimmers) would have higher levels of infectivity.

Park and Forst (2006) has attributed the co-regulation of motility and exoenzymes to the global regulator pathway, EnvZ-OmpR-FlhDC-FliA, in *Xenorhabdus nematophila*. During insect infection, levels of detectable *Xenorhabdus* cells in the hemocoel remain low until after insect death (Forst and Tabatabai, 1997). The bacteria become motile as the density of bacterial cells increases. This increased motility during stationary phase contributes to the dispersal of secondary metabolites throughout the insect cadaver, yielding the breakdown of tissues and the production of antibiotics throughout the hemolymph (Park & Forst, 2006). By effectively converting the insect cadaver into a “nutrient soup,” the global regulation of motility appears to play an essential role in the growth and development of the nematode host within the insect cadaver. However, FliA-global coregulation of motility and exoenzymes is not required for insect pathogenicity when introduced by injection (Park & Forst, 2006). Ciche and Ensign (2001) showed motility is not required for exiting the nematode host and

entering the insect cadaver, however, the transmission route of bacteria cells back into the nematode host is unknown. Based on these studies, I expected increased motility of the bacterial cells would positively influence the growth and development of the nematode and allow for better colonization or retention in the nematode host. Although symbiosis assays in this study were not completed *in vivo*, indications of motility were expected in the propagation of nematodes.

Bennett and Clarke (2005) determined the bacterial cell surface to be an important aspect of symbiosis or pathogenesis. This indicates alterations in the surface of the bacteria affect the surface-surface interactions between the bacteria and the immune cell or the nematode host. Bennett and Clarke obtained a symbiosis mutant that had altered motility properties from a surface property change. Sarua et al (2002) also showed surface alteration to cause sensitivity to changing environments in *E. coli*. Intact surface polysaccharides play a role in the natural resistance to strenuous environments. Leigh et al (1985) used calcofluor-white to identify *Rhizobium* mutants with altered surface properties. These mutants were defective in plant nodulation and the altered cell surface caused cells to not be recognized by the host plant during the infection process. Calcofluor-white binds to acidic residues in the exopolysaccharides of different bacterial species and has been used to identify mutants defective in the production of exopolysaccharides (Leigh et al, 1985; Ramaswamy et al, 1997). Janicki and Tisa (Unpublished) applied this method to examine cell surface properties in *Photorhabdus*. *P. temperata* secondary phase cells bind calcofluor while primary phase cells do not (Janicki & Tisa, Unpublished). Because the dye indicates alteration in cell surface, I hypothesized primary phase calcofluor-binding cells would be defective in symbiosis similar to secondary phase cells

and exhibit altered virulence. If this model were true, a calcofluor-binding assay would potentially be a quick screen for symbiosis or virulence defects. Based on my results, the significance of calcofluor-binding is inconclusive. Calcofluor-binding shows no correlation to symbiosis defects, however, one calcofluor-binding pathogenesis mutant was identified. Although this may not be a quick screen for pathogenesis/symbiosis mutants, it was an effective way of narrowing down to 11 mutants of interest from the transposon library.

With 96 mutants screened for pathogenesis and symbiosis, a majority of the transposon mutant library remains untouched in these fields. As these are labor-intensive screens, screening through the entire mutant library would not be cost-effective. Thus, new means of examining the transposon library are required to increase the effectiveness of the process. Based on the results from this study, new screens of the mutant library could potentially locate pathogenesis or symbiosis mutants. The entire transposon library is currently being screened for antibiotic production against indicator strains (Hurst & Tisa, Unpublished). The findings from this screen could potentially identify pathogenesis or symbiosis mutants. In my study, this link was particularly true for two pathogenesis mutants (UNH2033 and UNH1307), which were defective in antibiotic activity. These results suggest that this approach is feasible. Another screen capable of finding potential pathogenesis mutants is the hemolysis activity assay on blood agar plates, which is easily seen in a high-through put screen. Several of my confirmed mutants with delayed virulence were totally defective hemolysis activity, supporting the potential of this approach.

Insect Mortality Screen indicate all of the Mutants Tested were Virulent

For screening purposes, mutant cells were directly injected into larvae of the insect-host model, *G. mellonella* (Greater Wax moth). With a well-characterized immune response, *G. mellonella* is one of the most widely used host model systems to study *Photorhabdus* pathogenesis (Waterfield et al, 2009). Although not a natural means of infection, direct inoculation was cost-effective to quickly screen mutants for pathogenic traits and deliver a known amount of cells directly into the hemocoel of the wax moth larvae. Death of larvae that was attributed to *Photorhabdus* could be clearly seen as the white body turns a reddish-brown, rather than black due to an immune response. All 96 mutants caused insect mortality.

Photorhabdus is extremely virulent to a broad range of insects and has a myriad of virulence factors including insecticidal toxins and extracellular hemolysins (Waterfield et al, 2009). Analysis of *Photorhabdus* genome revealed the presence of genes encoding proteins similar to virulence factors in a wide range of mammalian pathogens (Duchard et al 2003; ffrench-Constant et al, 2000; Forst & Clarke, 2002). With so many redundant means of virulence, a complete knockout of pathogenicity by transposon mutagenesis was not seen, nor expected. To the best of my knowledge, a nonpathogenic mutant has never been attained in the *Photorhabdus* system. To truly compare virulence, the dose of infection was standardized for all mutants and parental wild-type control. Much of virulence is attributed to the rapid replication of bacterial cells in the insect host (Waterfield et al, 2009). However, growth rates of the mutants tested were similar to the parental wild-type and 4 mutants consistently showed an altered mortality rate at varied dosages (Figure 4). The dose dependent response of

infection indicates virulence to be directly related to the number of cells injected, and that these mutations altered *P. temperata* virulence.

All Screened Mutants were Capable of Nematode Symbiosis

Motility and calcofluor-binding mutants were screened for their symbiosis capabilities on lipid agar plates. I predicted that motility defective mutants including nonmotiles would be defective symbiosis by altering the competitive fitness of each mutant similarly to insect mortality. Due to an altered cell surface, I also expected calcofluor-binding capabilities to result in symbiosis defects. Although the initial screen indicated two mutants to be defective, further verification experiments indicate that all of the mutants were capable of forming a symbiosis. The ability to support the growth, development, and reproduction of *H. bacteriophora* was clearly seen as a white mass of nematodes (Figure 5). Although symbiosis was observed, bacterial retention numbers and nematode yield were not determined quantitatively. The defective result was most likely due to the dryness of the plates over a 21-day incubation. These screening experiments should be repeated and examined for quantitative effects. Although symbiosis occurred in all cases tested, verification experiments with individual lipid agar plates showed two mutants with altered capabilities. UNH5832 exhibited an accelerated rate of symbiosis formation, while UNH6427 showed a delayed rate.

Although this screening determined symbiosis mutants, further studies are required. While a mass of nematode growth is indicative of symbiosis capabilities, observations are mostly qualitative. A more quantitative method to

further identify symbiosis mutants would be useful. This method could help determine rates of symbiosis, as well as efficiency of symbiosis by quantitatively determining nematode propagation. Additionally, screened mutants should also be used for preference and retention studies. Preliminary preferential studies have shown *H. bacteriophora* to preferentially form symbiosis with wild-type *P. temperata* NC19 when plated with other wild-type strains (Gately and Tisa, unpublished). The use of other nematodes in these screening procedures would help identify genes involved in nematode specificity. Continued studies will show nematode preference of parental wild-type or mutant cells. Retention experiments completed so far indicate the retention of primary phase wild-type (Gately and Tisa, Unpublished). These experiments entail the homogenation of surface-sterilized nematodes grown on mutants of interest and determining viable cell numbers to indicate the retention of mutant cells in the nematode host. These future experiments will help support symbiosis results in my study.

Motility is not related to the Infection of Invertebrate Hosts

When choosing mutants to screen for insect mortality, I expected motility would play a role in the overall fitness of the mutant during pathogenesis. Though flagella formation or motility is not required for pathogenesis or symbiosis, motility does infer a competitive advantage in *Photorhabdus*. Motile cells outcompete nonmotile cells upon prolonged incubation within a host (Easom & Clarke, 2008). Motility has been linked to infections in many different genera including entering the host or adhering to host cells (Josenhans & Suerbaum, 2002).

In general all of the phenotypic motility groups were capable of pathogenesis and symbiosis. Enhanced pathogenesis was observed for nonmotile mutants (UNH2072), hyperswimmer mutants (UNH6290 and UNH9304), hyperswarmer mutants (UNH8322) and motility-defective mutants (UNH5832). Delayed pathogenesis was also observed for nonmotile mutants (UNH427 and UNH8678), hyperswimmer mutants (UNH7504), hyperswarmers (UNH8309, UNH1201, and UNH5006) and motility-defective mutants (UNH1307, UNH6441). With symbiosis, only hyperswarmer mutants (UNH1201, UNH8191, and UNH8178) and motility-defective mutants (UNH5832, UNH6427, and UNH8776) showed altered capabilities. Only mutants defective in motility were confirmed to have altered pathogenesis or symbiosis.

These mutants defective in motility caused either enhanced or delayed responses for pathogenesis and symbiosis. My results confirm previous findings that motility itself is not a factor for colonization of the invertebrate hosts (Easom & Clarke, 2008). Defective motility mutants were detected as swim-ring mutants. The mutants are motile, but form swim rings slowly and irregularly (Michaels, 2006). With *E. coli*, swim-ring formation is used to identify nonmotile and motility defective mutants (Adler, 1973). The motility-defective mutants are the result of a mutation in *E. coli* chemotaxis or motor genes. Nonmotile mutants are flagellar structural mutants.

My study disproved my original hypothesis. Although several defective motility mutants did have delayed pathogenesis, growth rate experiments showed no correlation to motility conferring fitness during pathogenesis. Nonmotile mutants were able to kill the invertebrate host at a rate similar to the

parental wild-type. This result indicates that motility is not required for insect pathogenesis under these conditions. Furthermore, mutant UNH5832 with greatly reduced motility killed the invertebrate host at a rate faster than the parental wild-type. With the exceptions of the designated defect, UNH5832 was very similar to parental wild-type in all other phenotypic properties (Table 3). One possible explanation for these results is that motility provides a competitive advantage under native infection conditions. For my study, an *in vitro* insect pathogenesis model system was used to determine virulence: larvae were directly injected with the bacteria. Motility may play a role in the infection through the nematode vector and the ability to provide growth conditions for nematode development. *In vivo* insect pathogenesis assays may show altered results with these mutants. Follow-up experiments with nematodes carrying mutant bacteria need to be performed to investigate this hypothesis.

Since *Photorhabdus* is a motile organism, there must be a competitive advantage to being so or else the trait would be lost (Easom & Clarke, 2008). To test if motility confers a competitive fitness in mutants a competitive assay between mutants and the parental wild-type could be performed. Recovery of the insect cadaver after a direct injection of the parental wild-type and mutant cells would indicate motility's role in infection. If motility does provide a competitive fitness, the most motile strain should outcompete an equally virulent counterpart.

Secondary phase characteristics for primary phase cell mutants

Several confirmed mutants had conflicting phase variation properties. *Photorhabdus* exists in two phenotypic phase variants, determined by several

phenotypic traits including dye absorption, and colonial and cellular morphology (Derzelle et al, 2004; Boemare et al. 1997; Akhurst, 1980). Though both phases are virulent, primary phase cells occur naturally in symbiosis with nematodes, and exhibit higher amounts of antibiotics, lipases, phospholipases, proteases, pigmentation and bioluminescence than the secondary phase variant (Gaudriault et al, 2008; Derzelle et al, 2004; Forst & Neilson, 1996).

My results suggest that dye-binding capabilities and colonial and cellular morphology are insufficient methods of determining *P. temperata* mutants phase state. UNH1307 and UNH2033 gave results similar to a wild-type secondary phase variant in a number of phenotypic assays, but showed a pathogenesis and symbiosis pattern similar to primary phase cells (Table 3). Though not as pronounced, UNH6441 also has several secondary phase traits, mostly dye-binding capabilities. Secondary phase wild-type cells exhibit more virulence than the primary phase variant, reaching an LT_{50} and LT_{100} at 35 h and 43 h, respectively. These values are lower than 38 h and 46 h for the LT_{50} and LT_{100} values of the primary phase wild-type, respectively. UNH1307 and UNH2033 both exhibited a delayed rate of pathogenesis, approximately 10-20 h slower than the primary phase parental wild-type. Most importantly, each mutant was able to successfully support the growth and development of the nematode host. This symbiosis capability truly defines both mutants as primary phase variants, although phenotypic traits indicate otherwise.

Calcofluor Mutant, UNH2033, Identified with Delayed Pathogenesis

Of the 11 mutants capable of binding Calcofluor-white, only one was identified as a pathogenesis mutant. Phenotypic characterization suggested

UNH2033 to be secondary phase because it does not bind dye on MacConkey or produce antibiotics (Table 3). However, this mutant is capable of supporting the growth and development of the nematode host. Furthermore, secondary phase cells are more virulent than primary phase cells. Previous work on the calcofluor-binding mutant, UNH2033, identified a match to the *P. temperata ngrA* gene (Janicki & Tisa, Unpublished). The *ngrA* gene is involved in nematode growth and reproduction (Ciche et al 2001). Ciche et al identified a mutant defective in the *ngrA* gene. This mutant retained all other primary phase characteristics. This gene identification suggests that the calcofluor-binding mutant is defective in its ability to interact with the nematode hosts. However, the recent symbiosis screening did not identify this mutant to be defective in symbiosis. This contradiction needs to be clarified and re-examined by further screens and genetic complementation. If the disruption of *ngrA* is responsible for the calcofluor-binding phenotype, symbiosis assays would need further verification. The significance of calcofluor-binding capabilities in *Photorhabdus* remains to be seen.

UNH1307 is a RNaseII mutant

Micheals (2006) originally identified UNH1307 as a mutant defective in motility and in a preliminary study showed delayed pathogenesis. Through arbitrary PCR, sequence analysis, and comparison to the *P. luminescens* genome, the disrupted gene of UNH1307 was identified as *E. coli yidA*, which is a protein with unknown function. With the available *P. temperata* genome sequence database, I determined the transposon-disrupted gene of UNH1307 to be *pte2811*,

or RNase II. As this genome sequence is still under construction, results were also compared with the closely related genome of *P. luminescens* (*plu2384*). These results were supported by a PCR approach, indicating the presence of the transposon within *pte2811*. End-point RT-PCR showed *pte2811* was not being expressed in UNH1307. These methods were not completed in the previous study. The discrepancy in genetic identification between studies is most likely due to the quality of sequencing results. Micheals obtained a 91% (162/178) similarity to the *P. luminescens* gene, while I obtained a 100% (574/574) match to *pte2811*. This *P. temperata* gene is a 91% (513/558) match to *plu2384* on a protein level.

Genetic complementation of UNH1307 proves pleiotropic effects of RNase II

The disrupted gene of UNH1307 was identified as *pte2811* (*plu2384*), or RNase II. To my knowledge, this is the first finding of RNase activity in the *Photorhabdus* system. I have shown that the disruption of RNase II in *P. temperata* leads to attenuated virulence, defective motility, decreased hemolysis activity and dye-binding capabilities, and defective antibiotic activity. This pleiotropic effect appears to be post-transcriptional and was proven by the genetic complementation of UNH1307 (Table 5). Potentially, RNase II degrades the message of a global regulator. This regulator would be a suppressor to the expression of the aforementioned traits. Within the RNase II mutant, the regulator is not undergoing degradation and is able to fully suppress these traits.

RNase II is a 3' to 5' exoribonuclease, which is an essential RNA-degrading multiprotein complex. This enzyme is involved in the maturation, turnover and quality control of RNA (Frazao et al, 2006). Expression of RNase II can be regulated by environmental conditions and differentially regulated at the

transcriptional and post-transcriptional levels (Barbas et al, 2009). RNase II has pleiotropic effects including a requirement for virulence in organisms such as *Shigella flexneri* and *E. coli*. Tsao et al, (2009) showed the homologue of RNase II, RNase R or *vacB*, to post-transcriptionally regulate several virulence and motility factors in the human pathogen, *Helicobacter pylori*. As this is a highly conserved protein throughout bacteria, it appears mRNA decay from RNase activity may regulate virulence factors across many genera. RNase R is a cold shock protein, sensitive to changes in temperature or pH, and particularly needed in stressful conditions. This indicates that the regulation of virulence and motility factors may play a role allowing cells to cope in strenuous environments (Tsao et al, 2009). Transcriptional profiling of the parental wild-type and UNH1307 would allow the specific regulated genes to be identified.

UNH6441 and UNH6427: Same Gene, Different Phenotypes

Discrepancies of this study lie within two mutants with defective motility. Mutants UNH6441 and UNH6427 were independently identified as pathogenesis and symbiosis mutants, respectively. Although these mutants exhibit different phenotypes, the sequencing of arbitrary PCR amplicons indicated the mutants to have the same disrupted gene, *pte2245*. Expression studies with end-point RT-PCR verified that neither mutant was expressing *pte2245*. Extensive analysis was completed, looking both up- and down-stream of *pte2245*, to determine if promoters had been affected. In both mutants, all surrounding genes were being expressed.

Further verification is needed to confirm all phenotypes, but there are possible explanations for these results. Southern hybridizations were able to confirm the random single-insertion of mini-Tn5 for UNH6427, however UNH6441 data was inconclusive. Repeating this procedure will indicate if UNH6441 has multiple insertions. Assuming a single insertion, the transposon could have truncated the protein, altering gene expression. It is also possible UNH6441 and UNH6427 are the same mutant. Originating from the same mutagenesis assay, these mutants could be genetically similar, if not identical.

To truly clarify this issue, genetic complementation is needed with *pte2245*. I expect that genetic complementation would not restore parental wild-type characteristics in both mutants. This procedure will prove causality for one mutant, while narrowing in on any discrepancies for the other. Genetic complementation has been attempted for mutants, UNH6441 and UNH6427. The wild-type gene *pte2245* has been amplified and cloned into a new construct, pHR2. Further work is needed to complete this complementation, however, results should resolve discrepancies between the two mutants.

Significance

By screening 96 transposon mutants, I have identified 5 mutants with altered pathogenesis and/or symbiosis. My results confirm previous reports that motility is not required for the infection of invertebrate hosts. This study suggests new screening methods of the transposon library to potentially identify additional pathogenesis mutants. My results suggest a re-evaluation of phase variation determination in *Photorhabdus* as traditional means have been shown

inefficient. Through the genetic complementation of UNH1307, I have shown RNase II to have pleiotropic effects in *Photobacterium*. RNase II regulates virulence, motility, dye-binding, antibiotic activity and hemolysis. This is the first data seen for RNase II in this system.

REFERENCES

- Adler, J.** 1973. "A method for measuring chemotaxis and use of the method to determine optimum conditions for chemotaxis by *Escherichia coli*." J Gen Microbiol. 74:77-91.
- Akhurst, R. J.** 1980. "Morphological and functional dimorphism in *Xenorhabdus* spp., bacteria symbiotically associated with the insect pathogenic nematodes *Neoaplectana* and *Heterorhabditis*." J Gen Microbiol. 121:303-309.
- Ansari, M.A., L. Tirry, and M. Moens.** 2002. "Entomopathogenic nematodes and their symbiotic bacteria for the biological control of *Hoplia philanthus* (Coleoptera: Scarabaeidae)." Biological Control. 28: 111-117.
- Bapteste, E., C. Brochier, Y. Boucher.** 2005. "Higher-level classification of the Archaea: evolution of methanogenesis and methanogens." Archaea. 1:353-363.
- Barbas, A., R. Matos, M. Amblar, E. Lopez-Vinas, P. Gomez-Puertas, and C.M Arraiano.** 2009. "Determination of key residues for catalysis and RNA-cleavage specificity: one mutation turns RNase II into a "super"-enzyme." Journal of Biological Chemistry. 284(31): 20487-20298.
- Barua, S., T. Yamashino, T. Hasegawa, K. Yokoyama, K. Torii, and M. Ohta.** 2002. "Involvement of surface polysaccharides in the organic acid resistance of Shiga Toxin-producing *Escherichia coli* O157:H7." Mol Microbiol. 43(3):629-40.
- Bennett, H. P. and D. Clarke.** 2005. "The pbgPE operon in *Photorhabdus luminescens* is required for pathogenicity and symbiosis." J. Bac. 187(1):77-84.
- Bode, H.B.** 2009. "Entomopathogenic bacteria as a source of secondary metabolites." Curr Opin Chem Biol. 13(2):224-230.
- Boemare, N.** 2002. "Biology, taxonomy and systematics of *Photorhabdus* and *Xenorhabdus*." In: Gaugler, R. editor. Entomopathogenic Nematology. New York: CAB International. p. 35-51.
- Boemare, N, J.-O. Thaler, and A. Lanois.** 1997. "Simple bacteriological tests for phenotypic characterization of *Xenorhabdus* and *Photorhabdus* phase variants." Symbiosis 22:167-175.

- Brillard, J., C. Ribeiro, N. Boemare, M. Brehelin.** 2001. "Two Distinct Hemolytic Activities in *Xenorhabdus nematophila* Are Active against Immunocompetent Insect Cells." *Applied and Environmental Microbiology*. 67(6):2515-2525.
- Brugirard-Ricaud, K., A. Givaudan, J. Parkhill, N. Boemaree, F. Kunst, R. Zumbihl, and E. Duchaud.** 2004. "Variation in the efforts of the Type III secretion system among *Photorhabdus* species as revealed by genomic analysis." *J. Bacteriol.* 186:4376-4381.
- Burnell, A and P. Stock.** 2000. *Heterorhabditis, Steinernema* and their bacterial symbionts lethal pathogens of insects. *Nematology*. 2(1): 31-42.
- Caetano-Annoles, G.** 1993. Amplifying DNA with arbitrary oligonucleotides. *PCR Methods Appl.* 3:85-92.
- Chattopadhyay, A., N. Bhatnagar, and R. Bhatnagar.** 2004. "Bacterial Insecticidal Toxins." *Critical Reviews in Microbiology*. 30(1):33-54.
- Ciche, T. A., S. Bintrim, A. Jorswill, and J. Ensign.** 2001. A Phosphoantethinyl Transferase Homolog Is Essential for *Photorhabdus luminescens* To Support Growth and Reproduction of the Entomopathogenic Nematode *Heterorhabditis bacteriophora*. *J Bacteriol.* 183:3117-3126.
- Ciche, T. and J. Ensign.** 2003. "For the Insect Pathogen *Photorhabdus luminescens*, Which End of a Nematode Is Out?" *Applied and Environmental Microbiology*. 69(4):1890-1897.
- Ciche, T., K. Kim, B. Kaufmann-Daszczuk, K. Nguyen, and D. Hall.** 2008. Cell Invasion and Matricide during *Photorhabdus luminescens* Transmission by *Heterorhabditis bacteriophora* Nematodes. *Applied and Environmental Microbiology*. 74(8):2275-87.
- Clarke, D.** 2008. "*Photorhabdus*: a model for the analysis of pathogenicity and mutualism." *Cell Microbiol.* 10(11):2159-2167.
- Clarke, D.J., and Dowds, B.C.A.** 1995. "Virulence mechanisms of *Photorhabdus* spp. Strain K122 toward wax moth larvae." *J. Invertebrate Pathology*. 66: 149-155.
- Costa, C., P. Girard, M. Brehelin, and R. Zumbihl.** 2009. "The emerging human pathogen *Photorhabdus asymbiotica* is a facultative intracellular bacterium and induces apoptosis of macrophage-like cells." *Infect. Immun.* 77(3):1022-30.
- Cowles, K., and H. Goodrich-Blair.** 2005. "Expression and activity of a *Xenorhabdus nematophila* haemolysin required for full virulence towards *Manduca sexta* insects." *Cell Microbiol.* 7(2): 209-19

- Daborn, P.J., N. Waterfield, C.P. Silva, C.P.Y. Au, S. Sharma, and R.H. ffrench-Constant.** 2002. "A single *Photorhabdus* gene, makes caterpillars floppy (mcf), allows *Escherichia coli* to persist within and kill insects." *Proc. Natl. Acad. Sci.* 99: 10742-10747.
- Daubin, V., M. Gouy, and G. Perriere.** 2002. "A Phylogenomic Approach to Bacterial Phylogeny: Evidence of a Core of Genes Sharing a Common History." *Genome Res.* 12: 1080-1090.
- Derzelle, S., S. Ngo, E. Turlin, E. Duchaud, A. Namane, F. Kunst, A. Danchin, P. Bertin, and J. Charles.** 2004. "AstR-AstS, a new two-component signal transduction system, mediates swarming, adaptation to stationary phase and phenotypic variation in *Photorhabdus luminescens*." *Microbiology.* 150(4):897-910.
- Dowds, B.C.A., and A. Peters.** 2002. "Virulence mechanisms." In: Gaugler, R. editor. *Entomopathogenic Nematology.* New York: CAB International. p. 79-93.
- Dowling, A., P. Daborn, N. Waterfield, P. Wang, C. Streuli, and R. ffrench-Constant.** 2004. "The insecticidal toxin Makes caterpillars floppy (Mcf) promotes apoptosis in mammalian cells." *Cell Microbiol.* 6(4):345-353.
- Duchard, E., C. Rusniok, L. Frangeul, C. Buchriesser, A. Givaudan,, S. Taourit, S. Bocs, C. Boursaux-Eude, M. Chanler, J.-F. Charles, E. Dassa, R. Deroose, S. Derzelle, G. Freyssinet, S. Gaudriault, C. Médigue, A. Lanois, K. Powell, P. Siguier, R. Vincent, V. Wingate, M. Zouine, P. Glaser, N. Boemare, A. Danchin, and F. Kunst.** 2003. The genome sequence of the entopathogenic bacterium *Photorhabdus luminescens*. *Nat. Biotechnol.* 21:1307 – 1313.
- Easom , C.A., and D.J. Clarke.** 2008. "Motility is required for the competitive fitness of entomopathogenic *Photorhabdus luminescens* during insect infection." *BMC Microbiology.* 8(168).
- Fan, Y., W. Fang, S. Guo, X. Pei, Y. Zhang, Y. Xiao, D. Li, K. Jin, M. Bidochka and Y. Pei.** 2007. "Increased Insect Virulence in *Beauveria bassiana* Strains Overexpressing an Engineered Chitinase." *Appl Environ Microbiol.* 73(1): 295-302.
- ffrench-Constant, R., N. Waterfield, P. Daborn, S. Joyce, H. Bennett, C. Au, A. Dowling, S. Boundy, S. Reynolds, and D. Clarke.** 2003. "*Photorhabdus*: towards a functional genomic analysis of a symbiont and pathogen." *FEMS Microbiology Reviews.* 26:433-456.
- Fitch, WM.** 1970. "Distinguishing homologous from analogous proteins." *Syst Zool.* 19:99-113.

- Forst, S., and D. Clarke.** 2002. "Bacteria-Nematode symbiosis." In: Gaugler, R. editor. *Entomopathogenic Nematology*. New York: CAB International. p. 57-74.
- Forst, S., and K. Neilson.** 1996. "Molecular biology of the symbiotic-pathogenic bacteria *Xenorhabdus* spp. and *Photorhabdus* spp." *Microbiology and Molecular Biology Reviews*. 60(1):41-40.
- Frazao, C., C. McVey, M. Amblar, A. Barbas, C. Vonnrhein, C. Arraiano, and M. Carrondo.** 2006. "Unravelling the dynamics of RNA degradation by ribonuclease II and its RNA-bound complex." *Nature*. 443:110-114.
- Gaudriault, S., S. Pages, A. Lanois, C. Laroui, C. Teyssier, E. Jumas-Bilak, and A. Givaudan.** 2008. "Plastic architecture of bacterial genome revealed by comparative genomics of *Photorhabdus* variants." *Genome Biol.* 9(7):R117
- Gerrard, J., S. Joyce, D. Clarke, R. French-Constant, G. Nimmo, D. Looke, E. Feil, L. Pearce, and N. Waterfield.** 2006. "Nematode symbiont for *Photorhabdus asymbiotica*." *Emerging Infect Dis* 12(10): 1562-1564.
- Gevers, D., K. Vandepoele, C. Simillion, Y. Van de Peer.** 2004. "Gene duplication and biased functional retention of paralogs in bacterial genomes." *Trends in Microbiology*. 12:4:148-154.
- Givaudan, A and A. Lanois.** 2000. "*flhDC*, the flagellar master operon of *Xenorhabdus nematophilus*: Requirement for motility lipolysis, extracellular hemolysis and full virulence in insects." *J. Bac.* 182(1):107-115.
- Gogarten, P., and L. Olendzenski.** 1999. "Orthologs, paralogs and genome comparisons." *Current opinion in genetics & development*. 9:630-636.
- Goodrich-Blair, H. and D.J. Clark.** 2007. "Mutualism and pathogenesis in *Xenorhabdus* and *Photorhabdus*: two roads to the same destination." *Molecular Microbiology*. 64:260-268.
- Graf, J., P. Dunlap and E. Ruby.** 1994. "Effect of transposon -induced motility mutation on colonization of the host light organ by *Vibrio fisheri*." *J. Bac.* 176(22):6986-6991.
- Guzman, L.-M., D. Belin, M. J. Carson, and J. Beckwith.** 1995. "Tight regulation, modulation and high level expression by vectors containing arabinose with P_{BAD} promoter." *J. Bacteriol.* 177(44):4121-4130.
- Hallem, E., M. Rengarajan, T. Ciche, and P. Sternberg.** 2007. "Nematodes, bacteria, and flies: A tripartite model for nematode parasitism." *Current Biology*. 17:898-904.

- Hogdson, M., B. Day, D.J. White, and L.S. Tisa.** 2003. "Effect of growth conditions on the motility of *Photorhabdus*." *Arch. Microbiol.* 180:17-24.
- Josenhans, C. and S. Suerbaum.** 2002. "The role of motility as a virulence factor in bacteria." *Int. J. Med. Microbiol.* 291:605-614.
- Joyce, S.A., R.J. Watson, and D.J. Clark.** 2006. "The regulation of pathogenicity and mutualism in *Photorhabdus*." *Current Opinion in Microbiology.* 9:127-132.
- Joyce, S.A., A. Brachmann, I. Glazer, L. Lango, G. Schwar, D. Clarke, H. Bode.** 2008. "Bacterial biosynthesis of a multipotent stilbene." *Angew Chem Int Ed Engl.* 47(10):1942-1945.
- Kanehisa, M. and A. Goto.** 2000. "KEGG: Kyoto Encyclopedia of Genes and Genomes." *Nucleic Acids Res.* 28: 27-30.
- Kavanagh, K, and E.P. Reeves.** 2004. "Exploiting potential for insect for *in vivo* pathogenicity testing of microbial pathogens." *FEMS Microbiology Reviews.* 28:101-112.
- Kavanagh, K., and E.P. Reeves.** 2007. "Insect and mammalian innate immune responses are much alike." *Microbe.* 12:596-599.
- Koonin EV.** 2005. "Orthologs, paralogs and evolutionary genomics." *Annu. Rev. Genet.* 39:309-338.
- Koonin E, and Y. Wolf.** 2008. "Genomics of bacteria and archaea: the emerging dynamic view of the prokaryotic world." *Nucleic Acids Res.* 36(21): 6688-6719.
- Leigh, J., E. Signer, and G. Walker.** 1985. "Exopolysaccharide-deficient mutants of *Rhizobium meliloti* that form ineffective nodules." *PNAS.* 82(18) 6231-6235.
- Lerat, E., V. Daubin, and N. Moran.** 2003. "From gene trees to organismal phylogeny in prokaryotes: The case of the α -Proteobacteria." *PLoS Biology.* 1(1):101-109.
- Lerat, E., V. Daubin, H. Ochman, and N. Moran.** 2005. "Evolutionary origins of genomic repertoires in bacteria." *PLoS Biology* 3(5):807-813.
- Markowitz, Victor, E. Szeto, K. Palaniappan, Y. Grechkin, K. Chu, I. Chen, I. Dubachak, I. Anderson, A. Lykidis, K. Mavromatis, N. Ivanova, and N. Kyrpides.** 2008. "The integrated microbial genomes (IMG) system in 2007: data content and analysis tool extensions." *Nucleic Acids Res.* 36:528-533.

- Marokhazi, J., N. Waterfield, G. LeGoff, E. Feil, R. Stabler, J. Hinds, A. Fodor and R.H. French-Constant.** 2003. "Using a DNA microarray to investigate the distribution of Insect virulence factor in strains of *Photorhabdus* bacteria." *J. Bacteriol.* 183:4648-4656.
- Mavrodi, D., J. Loper, I. Paulsen, and L. Thomashow.** 2009. "Mobile genetic elements in the genome of the beneficial rhizobacterium *Pseudomonas fluorescens* Pf-5." *BMC Microbiol.* 9: 8.
- Micheals, B.** 2006. "Genetics and physiology of motility by *Photorhabdus* spp." Ph.D. Thesis, The University of New Hampshire, Durham, NH.
- Micheals, B., R. Jakobek, E. Janicki, and L.S. Tisa.** 2004. "Identification of *Photorhabdus temperata* Motility Mutants and Their Physiological Properties." Abstr.I-042, *In* Abstracts of the 104th General Meeting of the American Society for Microbiology 2004. ASM, Washington, D.C. (New Orleans, LA).
- Minoru, Kanehisa, M. Araki, S. Goto, M. Hattori, M. Hirakawa, M. Itoh, T. Katayama, S. Kawashima, S. Okuda, T. Tokimatsu, Y. Yamanishi.** 2008. KEGG for linking genomes to life and the environment. *Nucleic Acids Res.* 36: 480-484.
- Moriya, Y., M. Itoh, S. Okuda, A. Yoshizawa, and M. Kanehisa.** 2007. "KAAS: an automatic genome annotation and pathway reconstruction server." *Nucleic Acids Res.* 35:182-185
- Mulkijanian, A., E. Koonin, K. Makarova, S. Mekhedov, A. Sorokin, Y. Wolf, A. Dufresne, F. Partensky, H. Burd, and D. Kaznadzey.** 2006. "The cyanobacterial genome core and the origin of photosynthesis." *Proc. Natl Acad. Sci. USA.* 103:13126-13131.
- Murray, M.G. and W.F. Thompson.** 1980. "Rapid isolation of high molecular weight plant DNA." *Nucleic Acids Res.* 8: 4321-4325.
- O'Toole, G., L. Pratt, P. Watnick, D. Newman, V. Weaver, and R. Kolter.** 1999. "Genetic approaches to study of biofilms." *Meth Enzymol.* 310: 91-109.
- Park, D., and S. Forst.** 2006. "Co-regulation of motility, exoenzyme and antibiotic production by the EnvZ-OmpR-FliHDC-FliA pathway in *Xenorhabdus nematophila*." *Mol Microbiol.* 61(6):1397-1412.
- Ramaswamy, S., M. Dworkin, and J. Downard.** 1997. "Identification and characterization of *Myxococcus xanthus* mutants deficient in calcofluor white binding". *J. Bacteriol.* 179(9): 2863-2871.
- Southern, E. M.** 1975. "Detection of specific sequences among DNA fragments separated by gel electrophoresis." *J. Mol. Biol.* 98(3): 503-517.

- Stecher B, Barthel M, Schlumberger MC, Haberli L, Rabsch W, Kremer M, Hardt W-D.** 2008. "Motility allows *S. typhimurium* to benefit from the mucosal defence." *Cell Microbiol.* 10:1166-1180.
- Syed, K., S. Beyhan, N. Correa, J. Queen, J. Liu, F. Peng, K. Stachell, F. Yildiz, and K. Klose.** 2009. "The *Vibrio cholerae* flagellar regulatory hierarchy controls expression of virulence factors." *Journal of Bacteriology.* 191(21):6555-6570.
- Tailliez, P., C. Laroui, N. Ginibre, A. Paule, S. Pages and N. Boemare.** 2009. "Phylogeny of *Photothabdus* and *Xenorhabdus* based on universally conserved protein-coding sequences and implications for the taxonomy of these two genera..." *Int J Syst Evol Microbiol.*
- Tounsi, S., M. Blight, S. Jaoua, and A. Lima Pimenta.** 2006. "From insects to human hosts: Identification of major genomic differences between entomopathogenic strains of *Photothabdus* and the emerging human pathogen *Photothabdus asymbiotica*." *International Journal of Medical Microbiology.* 296(8):521-530.
- Tsao, MY., TL. Lin, PF. Hsieh, and JT. Wang.** 2009. "The 3'-to-5' exoribonuclease (encoded by HP1248) of *Helicobacter pylori* regulates motility and apoptosis-inducing genes." *Journal of Bacteriology.* 191(8):2691-2702.
- Tyson, G., J. Chapman, P. Hugenholtz, E. Allen, R. Ram, P. Richardson, V. Solovyev, E. Rubin, D. Rokhsar, and J. Banfield.** 2004. "Community structure and metabolism through reconstruction of microbial genomes from the environment." *Nature.* 43:428-37.
- Venter, J., K. Remington, J. Heidelberg, A. Halpern, D. Rusch, J. Eisen, D. Wu, I. Paulsen, K. Nelson, W. Nelson.** 2004. "Environmental genome shotgun sequencing of the Sargasso Sea." *Science.* 304:6674.
- Waterfield, N., T. Ciche and D. Clarke.** 2009. "*Photothabdus* and a host of hosts." *Annu. Rev. Microbiol.* 63:557-74.
- Weisburg, W., S. Barns, D. Pelletier, and D. Lane.** 1991. "16S Ribosomal DNA amplification for phylogenetic study." *J. Bact.* 173(2):697-703.
- Yeung P.S., and K.J. Boor.** 2004. Epidemiology, pathogenesis, and prevention of food borne *Vibrio parahaemolyticus* infections. *Food-borne Pathog Dis.*1(2):74-88.
- Yooseph S., G. Sutton, D. Rusch, A. Halpern, S. Williamson, K. Remington, J. Eisen, K. Heidelberg, G. Manning, and W. Li.** 2007. "The Sorcerer II Global Ocean Sampling expedition: expanding the universe of protein families." *PLoS Biol.* 5:e16.

APPENDIX

FOREWORD

The following report was part of the coursework in Applied Bioinformatics at the University of New Hampshire. The purpose of this project was to identify orthologs involved in virulence in a core group of species from the *Photorhabdus* and *Xenorhabdus* genera. This project utilized the draft genome sequence of *P. temperata* and several other unpublished genomes with permissions. As the draft genome is still under reconfiguring, this work may be seen as currently incomplete. Though this project utilizes *P. temperata* and several closely related species, a different approach was taken. Rather than identifying virulence genes based on molecular and phenotypic characterizations, this project aimed to identify genes by genomic comparisons.

A GENOMIC APPROACH TO IDENTIFYING VIRULENCE GENES INVOLVED IN INSECT PATHOGENESIS

Introduction

One of the most anticipated uses of comparative genomics is the possibility of determining an organism's physiological function based on gene content. With rapidly growing databases of fully sequenced prokaryotes, many diverse phenotypes are represented by closely and distantly related organisms alike. Many organisms with lifestyles that correlate to well-defined metabolic pathways have already been discovered and compared using genomics. For example, methanogens and photosynthetic microorganisms have been discovered and characterized based on the presence of methane-byproduct or photosynthetic gene pathways, respectively (Baptiste et al, 2005; Mulkidjanian et al, 2006). The genome-lifestyle connection is not as definitive for lifestyles where many diverse genes and pathways are associated. This is further complicated as any genome contains 10-15% of genes with uncharacterized function (Tyson et al, 2004; Venter et al, 2004; Yooseph et al, 2007). Pathogenic and symbiotic lifestyles exemplify this principle because the currently characterized genes are not solely responsible for their host associations. (Yeung et al, 2004). Genomics not only helps determine the potential lifestyle of an organism, but may also help target functional characterization of unknown genes that are shared by organisms of similar lifestyles.

Ortholog prediction is imperative in comparative genomics and is often

utilized in genome annotation, gene function characterization, evolutionary genomics, and in the identification of conserved regulatory elements (Koonin et al, 2008). Orthologs are defined as genes that have diverged due to a speciation event, whereas genes that diverge due to a gene duplication event within a genome are considered paralogs (Fitch, 1970). Experimental data confirms that orthologs have conserved function even across diverse and distantly related organisms, thus, orthologs are vital for their utilization in comparative analyses (Koonin, 2005). Function conservation in paralogs is more ambiguous due to different evolutionary potential when there are multiple gene copies within a genome. Many tools have been developed to differentiate orthologs from paralogs so that common ancestry and function can be used for a vast range of comparisons between close or distantly related organisms alike (Lerat et al, 2003).

Due to large diversity and phylogeny, prokaryotes present particular challenges for comparative genomic analysis. The biggest driving forces of prokaryotic evolution are horizontal gene transfer (HGT), gene loss, and gene duplication (Gevers et al, 2004; Lerat et al, 2003). Gene acquisition from distant foreign lineages occurs frequently within bacterial genomes, greatly shaping evolutionary processes. In addition to vertical transmission, from parent to offspring, genes may also undergo horizontal transmission to genomes of other genera within a similar niche (Lerat et al, 2003). This type of transfer has been responsible for new functions and species, spreading biological processes such as virulence, and possibly playing a considerable role in the origin of eukaryotes (Eisen, 2000; Gogarten and Olendzenski, 1999). The consequent functional

divergence of gene duplicates also gives rise to broadening diversity of organismal function. Although content varies, prokaryotic genomes have a considerable portion of homologs within a genome. However, once selective environmental pressures cease, duplicates, as well as extraneous ancestral genes, can quickly be lost or excised (Gevers et al, 2004).

Small subunit ribosomal RNA (SSU rRNA), most commonly used for constructing organismal phylogeny, is believed to be conserved and ubiquitous among organisms. However, the sole use of this one gene to determine organismal phylogeny is insufficient (Lerat et al, 2003; Daubin et al, 2002). Although this gene is well conserved, using SSU rRNA to infer phylogeny assumes a constant evolutionary clock among genomes and only provides information on ancient divergence. Utilizing a larger set of orthologous genes would allow an analysis of recent evolutionary divergence by HGT, and the reevaluation of the relationships between genomes. Widespread orthologs, present in single copies, have been shown to undergo HGT at relatively low rate, providing a core set of genes with similar evolutionary histories (Daubin et al, 2002). By examining this core set of genes, a new phylogeny could be determined by identifying the ancestral genes as well as relatively recent acquisitions (Lerat et al, 2005; Gogarten and Olendzenski, 1999; Daubin et al, 2002).

Databases focusing on sequence analysis incorporate orthologs to compare known genomes and protein function to newly sequenced genomes. These databases predict function and phylogeny but lack the user interface to

provide tangible information to the user. The Kyoto Encyclopedia of Genes and Genomes (KEGG) allows for each access to predicted function in user-friendly biological pathways (Kanehisa, 2000). Through the KEGG automatic annotation server (KAAS), KEGG associates genes in a genome of interest to orthologous genes in genomes within the KEGG database (Moriya, 2007). The KEGG associated genes are combined with databases on enzyme function, chemical compounds, and phylogeny to create a visual representation of a biochemical pathway. These pathways range from metabolism, genetic information processing, signal transduction, and virulence (Minoru, 2008). Visually representing the interaction of genes with chemical compounds allows for the determination and efficient interpretation of function based on genome content.

The family *Enterobacteriaceae*, of the subgroup of Proteobacteria, consists of important model organisms, well understood gene functions, and is dense in fully sequenced genomes (Lerat et al, 2003; Clarke, 2008). This family includes the closely related genera *Photorhabdus* and *Xenorhabdus*, both of which have nearly identical complex life cycles. As entomopathogens, these bacteria are extremely virulent to a wide array of insects, all while maintaining a specific mutualism with nematodes from the family *Heterorhabditidae* and *Steinernematidae*, respectively (Goodrich-Blair, H and D. Clarke, 2007). With the demand of natural insecticides at an all time high, a further understanding of the natural insect virulence aspect of this lifecycle is necessary. The purpose of this study was to identify orthologs with common traits and physiological functions of virulence. By comparing genomic content of several pathogenic microbial species, novel and conserved virulence genes may be obtained.

Methods

Ortholog Determination and Analysis Genome sequences for genomes of interest were gathered from private and public databases (IMG) (Makowitz et al, 2008). Each protein was blasted against itself and all proteins in the genomes of interest. The bitscore was then used by the reciprocal Lerat method (Lerat et al, 2005) with a 0.3 threshold to determine orthology.

Two Perl scripts were created to sort the ortholog data; Group.pl searches for families containing genes from all the genomes while Only.pl searches for families containing genes unique to a specified group of genomes. Known functions were added to the output of genome name and IMG gene object identifier by Anotate.pl, which adds the protein name and locus tag by searching the genome protein file. Results were analyzed for potential genes of interest.

Phylogenetic Panortholog Trees Panorthologs were found using the only.pl program and aligned using Clustal. Phylip was used to create a most likely and maximum parsimony tree for each aligned panortholog. A most likely and maximum parsimony consensus tree was determined from the set using Consense. *Bacillus thuringiensis* was set as the outgroup for this analysis.

KEGG Annotation and Analysis KEGG Automatic Annotation Server (KAAS) was used to find associated KEGG genes from the reference sequence (ypp, plu, spe, pfo, eco, ecj, stm, sfl, ent, sdy, vch, vfi, btk, pae, ngo, bam, cje, gme, rco, atu, zmo, sac, spr, lca, mtc, fal, cca, baf, tth) for all genomes of interest (Moriya et al, 2007). The resulting KO list was used by Keggs.pl, created to take the KO lists of

multiple genomes and show presence or absence in each genome. Keggs.pl also accessed http://www.genome.jp/dbget-bin/www_bget?ko+<KO> for basic information on each KO number. The output was then sorted and analyzed using Microsoft Excel to search for genes of interest.

Results

Genomes of interest chosen based on taxa and lifestyle To determine orthologs exhibiting similar traits and physiological function of virulence, ten genomes were chosen for analysis based on phenotypes and related taxa. The core set of genomes included *Photorhabdus* spp. (*P. temperata*, *P. asymbiotica*, *P. luminescens*) and the closely related *Xenorhabdus* spp. (*X. bovienii*, *X. nematophila*). Other genomes included other gram-negative bacteria; the pathogen *Yersinia pestis*, a *Serratia* isolate from *Cenrhabditis briggsiae* (SCBI), and *Escherica coli*. Two genomes (*Bacillus thuringiensis*, *Pseudomonas fluorescens*) were chosen to represent outgroups. Primary analysis included the construction of a 16S phylogenetic tree, as well as basic examination of genome content and KEGG associated genes (Figure 1). Though species have different lifestyles, all contain a similar sized genome. Orthologs were distinguished to determine homologous genes of interest, separated by a speciation event. The ten genomes contained 3869 orthologs and 246 panorthologs.

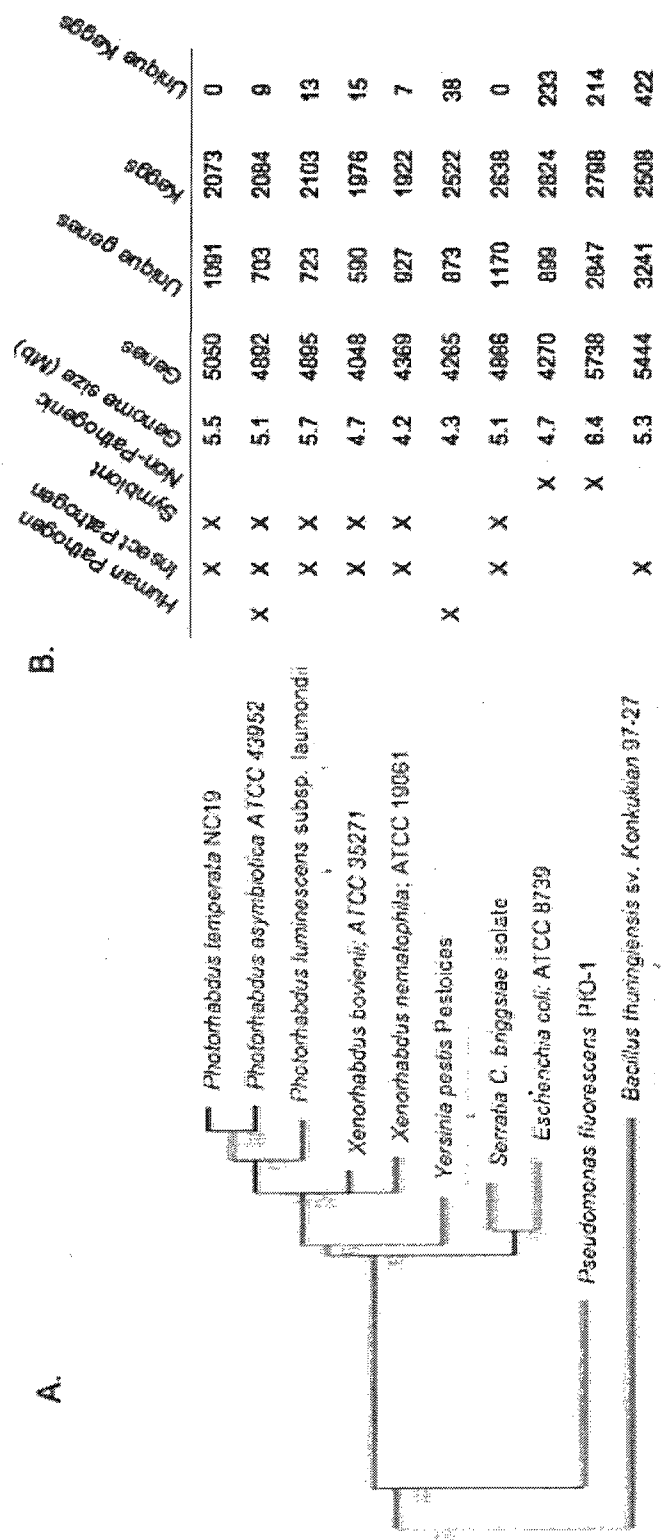


Figure 15. Genomic comparisons of 10 genomes of interest. (A) Constructed phylogeny tree based on 16S rRNA. (B) Primary analysis and comparisons of genome content.

Unique orthologs were determined within sets of genomes To determine orthologs unique to specific taxa or lifestyle, the 10 genomes of interest were categorized into groups (Figure 16). The 7 groups included (1) the in-group (*P. temperata*, *P. asymbiotica*, *P. luminescens*, *X. bovienii*, *X. nematophila*, *Y. pestis*, SCBI, *E. coli*), (2) *Photorhabdus* and *Xenorhabdus* spp., (3) *Photorhabdus* spp., (4) *Xenorhabdus* spp., (5) human pathogens (*P. asymbiotica*, *Y. pestis*), (6) insect pathogens (*P. temperata*, *P. asymbiotica*, *P. luminescens*, *X. bovienii*, *X. nematophila*, SCBI, *B. thuringiensis*), and (7) nematode symbionts and insect pathogens (*P. temperata*, *P. asymbiotica*, *P. luminescens*, *X. bovienii*, *X. nematophila*, SCBI). Through the use of the BLAST program from NCBI, the majority of these orthologs were found to be proteins of unknown function. As seen in Figure 2, this is particularly true of *Photorhabdus* spp.. Because of this uncharacterized function, most of the data could not be analyzed. Genomic groups were examined for known genes of interest associated with virulence (Table 6). Several known virulence factors were identified including multiple toxin complex proteins unique to *Xenorhabdus* and *Photorhabdus* spp. Other known unique orthologs included a chitin-binding protein and a hemolysin from insect pathogens and pathogens/symbionts, respectively.

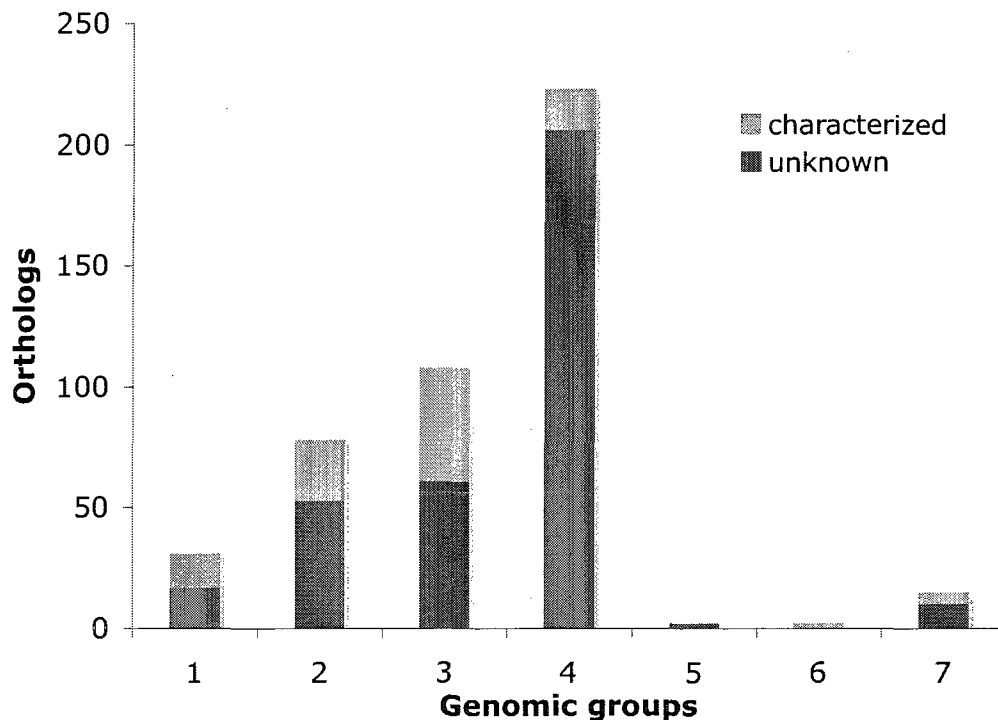


Figure 16. Orthologs unique to specified genomic groups and further determined as proteins of characterized or unknown functions. Group 1: In group; 2: *Xenorhabdus* spp. and *Photorhabdus* spp.; 3: *Xenorhabdus* spp.; 4: *Photorhabdus* spp.; 5: human pathogens; 6: insect pathogens; 7: symbionts and insect pathogens.

Table 6. Genes of interest unique to specified genomic groups (Fig. 2) and reference gene of *P. luminescens*. Note*: hypothetical protein.

Genomic Group	Gene	Reference
2 <i>Xenorhabdus/Photorhabdus</i> spp.	Insecticidal toxin complex protein TccA2	plu2460
	Insecticidal toxin complex protein TccB2	plu2459
4 <i>Photorhabdus</i> spp.	Insecticidal toxin complex protein TcaZ	plu0514
	Insecticidal toxin complex protein TcdA5	plu0971
	Virulence sensor protein BvgS precursor	plu2284
6 Insect Pathogen	Chitin-binding protein	plu2352*
7 Symbionts/Pathogens	hemolysin phIA	plu0316

Orthologous groups inferred phylogeny Although a phylogenous tree of the 10 genomes was created based on 16S, this method is limited to a single conserved gene. To examine a larger and more recent degree of divergence, orthologous groups were used to infer a more comprehensive phylogeny. Consensus trees of the 246 panorthologs were constructed for maximum likelihood and parsimony (Figure 17). This method resulted in two similar trees. Overall, results were similar to the constructed 16S phylogeny tree (Figure 15), with the exception of the relationship of *Y. pestis* and SCBI. Both consensus trees placed these organisms on the same clade with considerable certainty.

Virulence genes identified by KEGG content In addition to orthologs, genomes were analyzed to identify genes involved in particular pathways of interest. Associated KEGG genes for each genome was determined with KAAS, with a total of 3632 KEGGs. KEGGs of interest, identified to be in association of virulence, were classified as bacterial toxins and human disease (Table 7). This analysis allowed a comparison of functions for all genomes of interest.

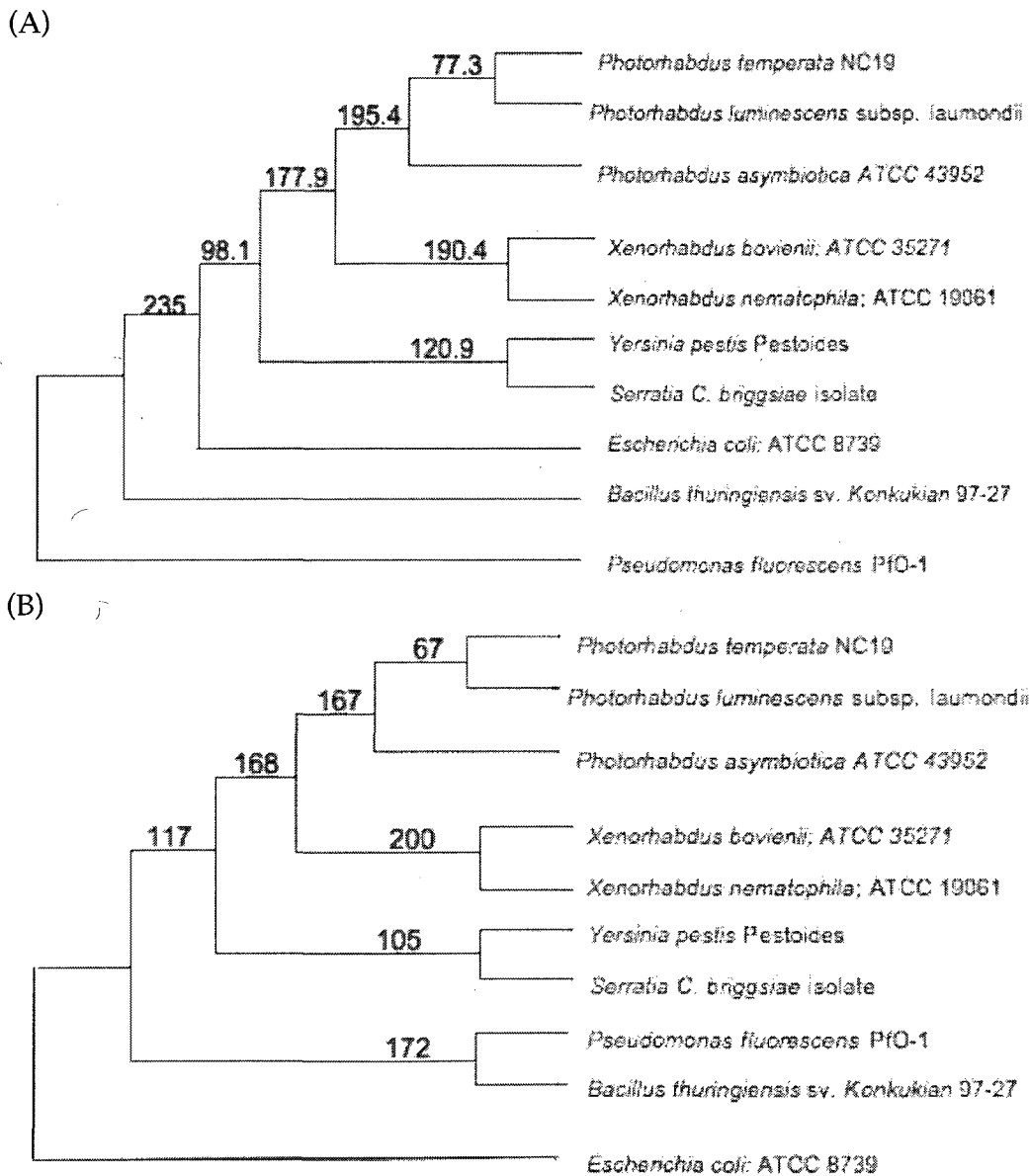


Figure 17. Proposed consensus phylogenetic trees based on 246 orthologs determined by (A) parsimony and (B) maximum likelihood. Values indicate number of orthologous trees in agreement.

Table 7. The presence (+) or absence of KEGGs, classified as bacterial toxins or involved in human disease, in each genome. (Bt, *B. thuringiensis*; Ec, *E. coli*; Pf, *P. fluorescens*; SCBI, *Serratia C. briggsiae* isolate; Pa, *P. asymbiotica*; Pl, *P. luminescens*; Pt, *P. temperata*; Xb, *X. bovienii*; Xn, *X. nematophila*)

Kegg Name	Genome										Notes
	Bt	Ec	Pf	Yp	SCBI	Pa	Pl	Pt	Xb	Xn	
Bacterial toxins											
hlyIII	+	+	+	+	+			+			Haemolysin-III related
hlyIII	+	+	+	+	+			+			
hblD	+										Bacillus haemolytic enterotoxins
nheBC	+										nonhemolytic enterotoxin
slo	+										streptolysin O toxin
hblC	+										hemolytic enterotoxin
hblAB	+										
nheA	+										
hblD	+										
nheBC	+										
slo	+										
hblC	+										
hblAB	+										
nheA	+										
hlyE, clyA, sheA		+									haemolysin proteins; pore-forming toxin
hlyE, clyA, sheA		+									
hcnB			+								hydrogen cyanide synthase
hcnA			+								
hcnC			+								
hcnB			+								
hcnA			+								
hcnC			+								
tccC			+	+		+	+		+	+	Insecticidal toxin complex genes
tccC			+	+		+	+		+	+	
shlB, hhdB			+	+	+	+	+	+	+	+	Haemolysin secretion/activation protein
shlA, hhdA			+	+	+	+	+	+	+	+	
shlB, hhdB			+	+	+	+	+	+	+	+	
shlA, hhdA			+	+	+	+	+	+	+	+	
ymt				+		+	+				murine toxin; transmission
ymt				+		+	+				
Human Diseases											
K08303	+	+	+	+	+	+	+	+	+	+	Infect. Diseases; Epithelial cell signaling
groEL, HSPD1	+	+	+	+	+	+	+	+	+	+	Metabolic Disorders; Type I diabetes
E1.15.1.1A, sodA, sodB, SOD2	+	+	+	+	+	+	+	+	+	+	Neurodegen. Diseases; Huntington's
E1.15.1.1C, sodC, SOD1	+	+		+	+			+			Neurodegen. Diseases; Amyotrophic lat.
crp	+	+	+	+	+	+	+	+	+	+	Infect. Diseases; V. cholerae pathogenic
acfD		+									Infect. Diseases; V. cholerae pathogenic
TROVE2, SSA2				+							Immune Disorders; Sys. lupus erythematosus
f1rA				+							Infect. Diseases; V. cholerae pathogenic
f1rC, f1eR				+							Infect. Diseases; V. cholerae pathogenic
f1rB, f1eS				+							Infect. Diseases; V. cholerae pathogenic
rtxA						+	+		+	+	Infect. Diseases; V. cholerae infection

Discussion

The purpose of this study was to identify orthologs with similar physiological functions of virulence. A 16S phylogenetic tree was constructed with related taxa of the focus group, *Photorhabdus* and *Xenorhabdus* spp. (Fig 1A). To obtain an accurate set of orthologs, this tree was designed to contain insect pathogens, nematode symbionts and human pathogens of the family *Enterobacteriaceae*. *B. thuringiensis* (Bt), a gram-positive insect pathogen, and *P. fluorescens*, a gram-negative asymbiotic nonpathogen, were chosen for outgroups. This tree served as the basis for all other comparisons of gene content (Fig. 1B). A particular issue with this set of genomes was access to well annotated genomes through public databases. Half of the genomes were either obtained with permission, or annotated on premises. These genomes, including *P. asymbiotica*, SCBI, *P. temperata*, and *Xenorhabdus* spp., contained fewer known protein functions than published genomes. In particular, *P. temperata* draft genome is still under analysis, filling gaps in 17 scaffolds.

For analysis of numerous orthologs, genomes were grouped according to taxa and particular phenotypes (Fig. 2). These genomic groups served as tools for the identification of functional orthologs unique to a specified grouping. Although most orthologs are unnamed proteins with uncharacterized functions, genes of interest were recognized (Table 6). A chitin-binding protein is one of the characterized orthologs that was found to be unique to insect pathogenicity. Chitin-binding proteins facilitate and increase the rate of chitin degradation by associating with chitinase. As chitin is a major component of an insect cuticle and the primary barrier against infection, increased degradation leads to

increased virulence (Fan et al, 2007). By grouping the *Photorhabdus* spp., 223 orthologs were found to be unique to this group. Three orthologs, of the 23 characterized proteins, were identified as being involved in virulence. These orthologs include insecticidal toxin complex proteins *tcaZ* and *tcdA5*, known factors of oral toxicity and the broad range of insects *Photorhabdus* spp. are capable of infecting (French-Constant et al, 2003). Other toxin complex proteins (tcc) were also found to be unique to *Xenorhabdus/Photorhabdus* spp. core.

Although not novel, the identification of these proteins associated with virulence, such as chitin-binding and toxin complex proteins, proves this method is capable of identifying virulence orthologs. With the majority (~90%) of identified orthologs having uncharacterized functions, further analysis is required to identify additional genes of interest to obtain novel virulence genes. This is particularly true of the five genomes unavailable through public databases, which are heavily uncharacterized.

In addition to function, orthologs may also be utilized to infer phylogeny. The use of ribosomal RNA to construct a phylogenetic tree is insufficient as it only represents ancient evolutionary divergence. A broad set of orthologs can infer the more recent divergence due to HGT or gene loss (Lerat et al, 2003). A total of 246 orthologous trees, one for every panortholog protein, were constructed for both parsimony and maximum likelihood (Fig. 4). Although sufficient results were obtained, running this program with nucleic acids could have maximized resolution. This is particularly true between species of the same genus.

Although very similar to the 16S tree, consensus trees based on orthology contain a significant difference, the relationship between *Y. pestis* and SCBI.

These two genomes, previously unknown to be closely related through 16S, were placed on the same branch in the constructed orthologous trees. Upon further examination, these genomes were seen to have 109 unique orthologs between them. Of the 53 characterized orthologs, two are known to be virulence factors. SCBI, like the focus group, is an insect pathogen and symbiont of Caenothabditid nematodes. *Y. pestis* has a much different lifestyle; in association with insects, it is primarily a human pathogen that is responsible for diseases such as the bubonic plague. *Y. pestis* genome was added due to studies suggesting horizontal gene transfer between *Y. pestis* and *Photorhabdus* spp. (Clarke, 2008). As all genomes have had long-term associations with insects, recent evolutionary convergence is possible.

Although orthologs provide great insight to relation and function of genes, further information can be obtained by examining genes involved in particular pathways. KEGG analysis provided the presence and absence of virulence genes involved in known pathways within each genome (Table 7). This data supports the findings of the phylogenetic trees, as the KEGG content of SCBI and *Y. pestis* are quite similar to each other. The differences with the outgroup *B. thuringiensis* is prominently seen, with very few overlaps of known bacterial toxins. Although Bt is a lethal insect pathogen, it is obvious the distant organism utilizes a different triad of virulence factors. Similarities among the focus group of *Xenorhabdus* and *Photorhabdus* spp. are evident, though discrepancies do exist. Most surprisingly are the numerous virulence KEGG pathways present in the nonpathogenic outgroup, *P. fluorescens*. Other species of *Pseudomonas* are pathogens, including human and plant, however *P. fluorescens* actually protects plants against disease (Mavrodi et al, 2009). It is possible these

virulence genes are contained in the genome due to ancestry though they are not expressed. This indicates a flaw in the method of solely using genomic data and not expression studies.

Through this study, an effective method of identifying virulence orthologs was determined. By distinguishing genes of known virulence, one can assume novel virulence genes can be found within proteins of unknown function. This study showed that inferring phylogeny from orthologs produces results based on ancestry as well as function. Although differences were seen, additional genomes for comparison are necessary to verify significance. Overall, the comparative genomic methods of this study have proven useful, however much further analysis is required.

Acknowledgements

I would like to thank my MIGHTY team members: Greg Schwendimann, Nick Beauchemin, and Brian Schuster. Thank you Feseha Abebe-Akele for helping and contributing annotated sequences. Also, thank you professors Louis Tisa, Kelley Thomas, and Dan Bergeron. Thank you to the University of Wisconsin for providing access to *Xenorhabdus* genomes.